2. Tateno C, Yoshizane Y, Saitou N, *et al.* Near completely humanized liver in mice shows human-type metabolic responses to drugs. Am J Pathol 2004;165:901–912.
3. Katoh M, Matsui T, Okamura H, *et al.* Expression of human phase II enzymes in chimeric mice with humanized liver. Drug Metab Dispos 2005;33:1333–1340.
4. Nishimura M, Yoshitsugu H, Yokoi T, *et al.* Evaluation of mRNA expression of human drug-metabolising enzymes and transporters in chimeric mouse with humanized liver. Xenobiotica 2005;35: 877–890.
5. Shi J, Fujieda H, Kokubo Y, *et al.* Apoptosis of neutrophils and their elimination by Kupffer cells in rat liver. Hepatology 1996;24: 1256–1263.
6. Warren A, Le Couteur DG, Fraser R, *et al.* T lymphocytes interact with hepatocytes through fenestrations in murine liver sinusoidal endothelial cells. Hepatology 2006;44:1182–1190.
7. Sato Y, Yamada H, Iwasaki K, *et al.* Human hepatocytes can repopulate mouse liver: histopathology of the liver in human hepatocyte-transplanted chimeric mice and toxicologic responses to acetaminophen. Toxicol Pathol 2008;36:581–591.
8. Meuleman P, Libbrecht L, De Vos R, *et al.* Morphological and biochemical characterization of a human liver in a uPA-SCID mouse chimera. Hepatology 2005;41:847–856.
9. Nonaka H, Tanaka M, Suzuki K, *et al.* Development of murine hepatic sinusoidal endothelial cells characterized by the expression of hyaluronan receptors. Dev Dyn 2007;236:2258–2267.
10. Katayama S, Tateno C, Asahara T, *et al.* Size-dependent in vivo growth potential of adult rat hepatocytes. Am J Pathol 2001;158: 97–105.
11. Ban D, Kudo A, Sui S, *et al.* Decreased Mrp2-dependent bile flow in the after-warm ischemic rat liver. J Surg Res 2009;153:310–316.
12. Mabuchi A, Wake K, Marlini M, *et al.* Protection by glycyrrhizin against warm ischemia-reperfusion-induced cellular injury and derangement of the microcirculatory blood flow in the rat liver. Microcirculation 2009;16:364–376.
13. Wisse E, Braet F, Duimel H, *et al.* Fixation methods for electron microscopy of human and other liver. World J Gastroenterol 2010;16:2851–2866.
14. Seglen PO. Preparation of isolated rat liver cells. Methods Cell Biol 1976;13:29–83.
15. Bolstad BM, Irizarry RA, Astrand M, *et al.* A comparison of normalization methods for high density oligonucleotide array data based on variance and bias. Bioinformatics 2003;19:185–193.
16. Eisen MB, Spellman PT, Brown PO, *et al.* Cluster analysis and display of genome-wide expression patterns. Proc Natl Acad Sci USA 1988;95:14863–14868.
17. Tateno C, Kataoka M, Utoh R, *et al.* Growth hormone-dependent pathogenesis of human hepatic steatosis in a novel mouse model bearing a human hepatocyte-repopulated liver. Endocrinology 2011;152:1479–1491.
18. Asahina K, Sato H, Yamasaki C, *et al.* Pleiotrophin/HB-GAM as a mitogen of rat hepatocytes and its role in regeneration and development of liver. Am J Pathol 2002;160:2191–2205.
19. Benjamini Y, Hochberg Y. Controlling the false discovery rate: a practical and powerful approach to multiple testing. J Roy Statist Soc Ser B 1995;57:289–300.
20. Utoh R, Tateno C, Kataoka M, *et al.* Hepatic hyperplasia associated with discordant xenogeneic parenchymal-nonparenchymal interactions in human hepatocyte-repopulated mice. Am J Pathol 2010;177:654–665.
21. Michael L. Laboratory Medicine: The Diagnosis in the Clinical Laboratory, New York, 2010.
22. Jensen FS, Skovgaard LT, Viby-Mogensen J. Identification of human plasma cholinesterase variants in 6,688 individuals using biochemical analysis. Acta Anaesthesiol Scand 1995;39:157–162.
23. Porter RK, Brand MD. Causes of differences in respiration rate of hepatocytes from mammals of different body mass. Am J Physiol 1995;269:R1213–R1224.
24. Maeno H, Ono T, Dhar DK, *et al.* Expression of hypoxia inducible factor-1alpha during liver regeneration induced by partial hepatectomy in rats. Liver Int 2005;25:1002–1009.
25. Tomoyori T, Ogawa K, Mori M, *et al.* Ultrastructural changes in the bile canaliculi and the lateral surfaces of rat hepatocytes during restorative proliferation. Virchows Arch B Cell Pathol Incl Mol Pathol 1983;42: 201–211.
26. Souza SC, Frick GP, Wang X, *et al.* A single arginine residue determines species specificity of the human growth hormone receptor. Proc Natl Acad Sci USA 1995;92:959–963.
27. Masumoto N, Tateno C, Tachibana A, *et al.* GH enhances proliferation of h-heps grafted into immunodeficient mice with damaged liver. J Endoclinol 2007;194:529–537.
28. Sandgren EP, Palmiter RD, Heckel JL, *et al.* Complete hepatic regeneration after somatic deletion of an albumin-plasminogen activator transgene. Cell 1991;66:245–256.
29. Dinchuk J, Hart J, Gonzalez G, *et al.* Remodelling of lipoproteins in transgenic mice expressing human cholesteryl ester transfer protein. Biochim Biophys Acta 1995;1255:301–310.

Toxicology Letters 214 (2012) 9–18

Contents lists available at SciVerse ScienceDirect

Toxicology Letters

journal homepage: www.elsevier.com/locate/toxlet

Chimeric mice with a humanized liver as an animal model of troglitazone-induced liver injury

Masakazu Kakuni[a], Mayu Morita[b], Kentaro Matsuo[b], Yumiko Katoh[a], Miki Nakajima[b], Chise Tateno[a], Tsuyoshi Yokoi[b,*]

[a] PhoenixBio Co., Ltd., Hiroshima 739-0046, Japan
[b] Division of Pharmaceutical Sciences, Faculty of Pharmaceutical Sciences, Kanazawa University, Kakuma-machi, Kanazawa 920-1192, Japan

HIGHLIGHTS

- Troglitazone (Tro) was withdrawn due to its association with severe liver injury.
- Orally administered Tro has never induced liver injury in experimental animals.
- The chimeric mice with a humanized liver reproduced Tro-induced liver injury.
- Possible factors that contribute to the Tro-induced liver injury were evaluated.
- This mouse model enables human hepatocytes to be examined in an *in vivo* environment.

ARTICLE INFO

Article history:
Received 11 April 2012
Received in revised form 31 July 2012
Accepted 2 August 2012
Available online xxx

Keywords:
Chimeric mouse with a humanized liver
Drug-induced liver injury (DILI)
Hepatotoxicity
Troglitazone
Glutathione

ABSTRACT

Troglitazone (Tro) is a thiazolidinedione antidiabetic drug that was withdrawn from the market due to its association with idiosyncratic severe liver injury. Tro has never induced liver injury in experimental animals *in vivo*. It was assumed that the species differences between human and experimental animals in the pharmaco- or toxicokinetics of Tro might be associated with these observations. In this study, we investigated whether a chimeric mouse with a humanized liver that we previously established, whose replacement index with human hepatocytes is up to 92% can reproduce Tro-induced liver injury. When the chimeric mice were orally administered Tro for 14 or 23 days (1000 mg/kg/day), serum alanine aminotransferase (ALT) was significantly increased by 2.1- and 3.6-fold, respectively. Co-administration of L-buthionine sulfoximine (10 mM in drinking water), an inhibitor of glutathione (GSH) synthesis, unexpectedly prevented the Tro-dependent increase of ALT, which suggests that the GSH scavenging pathway will not be involved in Tro-induced liver injury. To elucidate the mechanism of the onset of liver injury, hepatic GSH content, the level of oxidative stress markers and phase I and phase II drug metabolizing enzymes were determined. However, these factors were not associated with Tro-induced liver injury. An immune-mediated reaction may be associated with Tro-induced liver toxicity *in vivo*, because the chimeric mouse is derived from an immunodeficient SCID mouse. In conclusion, we successfully reproduced Tro-induced liver injury using chimeric mice with a humanized liver, which provides a new animal model for studying idiosyncratic drug-induced liver injury.

1. Introduction

Troglitazone (Tro) was the first thiazolidinedione used for treating of type II diabetes mellitus, but was withdrawn due to serious idiosyncratic liver injury. During the preclinical development of Tro, no study could predict the hepatotoxic effect of Tro in human (Watanabe et al., 1999). After the withdrawal of Tro from the market, numerous studies using animal models were performed to reproduce the hepatotoxicity of Tro, but almost all were unsuccessful (Bedoucha et al., 2001; Jia et al., 2000; Watanabe et al., 2000).

Ong et al. (2007) reported that the administration of Tro (30 mg/kg, *i.p.*) to heterozygous superoxide dismutase 2 (SOD2) knockout ($SOD2^{+/-}$) mice resulted in hepatocellular necrosis and increased serum alanine aminotransferase (ALT) levels, suggesting that SOD2, which is expressed mainly in the mitochondria, plays a crucial role in Tro-induced liver injury. However, other research group could not reproduce these results using the same

* Corresponding author at: Drug Metabolism and Toxicology, Faculty of Pharmaceutical Sciences, Kanazawa University, Kakuma-machi, Kanazawa 920-1192, Japan. Tel.: +81 76 234 4407; fax: +81 76 234 4407.
E-mail address: tyokoi@kenroku.kanazawa-u.ac.jp (T. Yokoi).

0378-4274/$ – see front matter © 2012 Elsevier Ireland Ltd. All rights reserved.
http://dx.doi.org/10.1016/j.toxlet.2012.08.001

heterozygous SOD2 knockout mice (Fujimoto et al., 2009). No further studies of *in vivo* animal models have been reported.

Because idiosyncratic liver injury is a human-specific toxic event, we surmised that previously established chimeric mice with a humanized liver (Tateno et al., 2004) might be useful as an animal model. In this study, we investigated whether Tro causes liver injury in a chimeric mouse with a humanized liver, which was derived from a urokinase-type plasminogen activator$^{+/+}$/severe combined immunodeficient transgenic (uPA$^{+/+}$/SCID mouse) mouse line. In this animal model, more than 75% of the mouse hepatocytes are replaced with human hepatocytes in which the human mRNAs and proteins expression levels and enzyme activities were evaluated (Katoh et al., 2004, 2005, 2007; Nishimura et al., 2005).

Tro undergoes metabolic activation by CYPs, in particular, the CYP3A4 isoform, to form reactive metabolites that bind covalently to proteins and nucleophiles, such as glutathione (GSH) and cysteine. Various reactive metabolites of Tro were identified as GSH conjugates (Tettey et al., 2001; Kassahun et al., 2001; He et al., 2004). The susceptibility of drugs metabolized to reactive intermediates is different between GSH-depleted animals and normal animals (T. Watanabe et al., 2003; Usui et al., 2011). Therefore, we expected that Tro would exhibit hepatotoxic effects under a GSH-depleted condition. L-Buthionine sulfoximine (BSO), a well-known inhibitor of GSH synthesis, was selected to investigate the relationship between the GSH conjugation ability and Tro-induced hepatotoxicity.

In the present study, we orally administered Tro for 14 or 23 days to chimeric mice with a humanized liver and reproduced liver injury. Subsequently, possible factors that were expected to contribute to the development of Tro-induced liver injury, such as drug-metabolizing enzymes, GSH, SOD2, and protein carbonyl contents, were evaluated.

2. Materials and methods

2.1. Chemicals

TRO was kindly provided by Daiichi Sankyo (Tokyo, Japan). L-Buthionine sulfoximine (BSO) and paclitaxel were purchased from Sigma (St. Louis, MO). ReverTra Ace was from Toyobo (Tokyo, Japan). Random hexamer, RNAiso, SYBR Premix Ex Taq, and ROX Reference Dye II were from Takara (Osaka, Japan). Recombinant human CYP2C8 and CYP3A4 expressed in baculovirus-infected insect cells and 6a-hydroxypaclitaxel were from BD Gentest (Woburn, MA). Dexamethasone and testosterone were from Wako Pure Chemical Industries (Osaka, Japan). 6b-Hydroxytestosterone was from Sekisui Medical (Tokyo, Japan). All primers were commercially synthesized at Hokkaido System Sciences (Sapporo, Japan). The polyclonal rabbit anti-human CYP2C8 antibody was from Nosan (Yokohama, Japan) and the polyclonal goat anti-CYP3A antibody (sc-30621) was from Santa Cruz Biotechnology (Santa Cruz, CA). All other chemicals were of analytical or the highest grade commercially available.

2.2. Generation of the chimeric mice with a humanized liver

The present study was conducted in accordance with the National Institutes of Health Guide for Animal Welfare of Japan, and the protocols were approved by the Institutional Animal Care and Use Committees of Kanazawa University (Kanazawa, Japan) and PhoenixBio Co., Ltd. (Hiroshima, Japan). The chimeric mice were generated by PhoenixBio. Briefly, commercially available cryopreserved human hepatocytes (5-year-old African-American male from BD Gentest) were transplanted into the spleens of uPA$^{+/+}$/SCID mice at approximately 3–4 weeks of age. At mice's age of 6–7 weeks, the monitoring of human albumin (h-Alb) concentration in blood was started and continued until the start of the study when the chimeric mice were 11–15 weeks old. Two microliters of blood was collected from tail vein of the mice once per week, and the concentrations of hAlb in the blood of the chimeric mice were determined by latex agglutination immunonephelometry to estimate the rate of replacement of mouse hepatocytes with human hepatocytes (RI: Replacement Index). The correlation between hAlb and the actual RI has been determined based on immunohistochemistry conducted with anti-human specific cytokeratin 8 and 18 antibodies (Tateno et al., 2004). The chimeric mice used in the present study were female, 11–15 weeks old, and exhibited concentrations of 8.0–14.9 mg/ml of hAlb or an RI of 75–92% at the start of the TRO administration (Table 1). The animals were housed in a controlled environment (temperature 23 ± 1 °C, humidity 57 ± 15%, and 12 h light/12 h dark cycle) in the institution's animal facility with *ad libitum* access to food and water.

2.3. Drug and/or BSO administration

The chimeric mice were orally administered Tro [250 mg/kg/10 ml, 500 mg/kg/ml or 1000 mg/kg/10 ml, suspended in 0.5% carboxymethylcellulose (CMC)] once daily for 14 (1000 mg/kg), 23 (1000 mg/kg) or 28 (250 and 500 mg/kg) days in a non-fasting condition, and 0.5% CMC was administered once daily as a control. BSO (10 mM) in sterilized tap water was also administered *via* drinking water alone or with Tro. Water bottle was changed twice a week during the BSO treatment. The dosing method was originally reported by T. Watanabe et al. (2003), in which 5–30 mM of BSO in drinking water had been confirmed to be stable for 15 days at 23 °C without light-shielded conditions. Pre-dosing blood samples were collected under isoflurane anesthesia to measure the initial serum ALT level. Twenty-four hours after the last Tro administration, the blood and livers were collected by exsanguination under isoflurane anesthesia. Serum ALT, aspartate aminotransferase (AST), bilirubin (total bilirubin: T-Bil, and direct bilirubin: D-Bil) and lactate dehydrogenase (LDH) levels were measured using FUJI DRI-CHEM (FUJIFILM, Tokyo, Japan). A portion of the liver was fixed in buffered neutral 10% formalin. The fixed samples were embedded in paraffin, sectioned at a thickness of 2 μm and stained with hematoxylin–eosin (H&E) for microscopic examination.

2.4. GSH level

Mouse livers were homogenized in ice-cold 5% sulfosalicylic acid using a glass homogenizer and centrifuged at 8000 × *g* at 4 °C for 10 min. The GSH concentration in the supernatant was measured as described previously (Tietze, 1969).

2.5. Glutathione S-transferase (GST) activity

GST activity was measured according to the method of Habig et al. (1974) with slight modifications. The incubation mixtures consisted of cytosol (0.1 ml) in 125 mM potassium phosphate buffer (pH 6.5) containing 1.25 mM GSH (0.8 ml) and 10 mM 1-chloro-2,4-dinitrobenzene in 40% ethanol (0.1 ml). The reaction mixture was incubated at 25 °C for 10 min and monitored at 340 nm.

2.6. SOD2 activity

SOD2 activity was measured using a Superoxide Dismutase Assay kit (Cayman Chemical, Ann Arbor, MI). The method utilizes tetrazolium salt to quantify the superoxide radicals generated by xanthine oxidase and hypoxanthine. The standard curve was generated using a quality controlled SOD standard in the kit. SOD2 activity was determined in the presence of potassium cyanide to inhibit SOD1 activity.

2.7. Protein carbonyl content

Plasma protein carbonyl content was measured using an OxiSelect Protein Carbonyl ELISA kit (Cell Biolabs, Tokyo, Japan) as described previously (Yoshikawa et al., 2009).

2.8. Real-time reverse transcription (RT)-PCR

Total hepatic RNA was isolated using RNAiso according to the manufacturer's instructions. Human CYP2C8, CYP3A4, SULT1A1, UGT1A1 and GAPDH mRNA levels were quantified by real-time RT-PCR. Total RNA (4 μg) and 150 ng random hexamer were mixed and incubated at 70 °C for 10 min. An RNA solution was added to a reaction mixture that contained 100 units of ReverTra Ace, reaction buffer and 0.5 mM dNTPs in a final volume of 40 μl. The reaction mixture was incubated at 30 °C for 10 min, 42 °C for 1 h, and then heated at 98 °C for 10 min to inactivate the enzyme. Real-time RT-PCR was performed using the Mx3000P (Stratagene, La Jolla, CA). The PCR mixture contained 1 μl of template cDNA, SYBR Premix Ex Taq solution, and 10 pmol of sense and antisense primers. The human-specific primer sequences used in this study are shown in Table 2. The amplified products were monitored directly by measuring the intensity of the SYBR Green I dye (Molecular Probes, Eugene, OR) that binds to the PCR amplified double-stranded DNA.

2.9. Immunoblot analysis

SDS-polyacrylamide gel electrophoresis and immunoblot analysis of human CYP2C8 and CYP3A were performed according to Katoh et al. (2004). The liver microsomes (2 or 20 μg) were separated on 10% polyacrylamide gel and transferred electrophoretically to a polyvinylidene difluoride membrane. Recombinant human P450s were applied as standards. Biotinylated anti-rabbit or goat IgG and a Vectastain ABC kit (Vector Laboratories, Burlingame, CA) were used for diaminobenzidine staining. It was confirmed that the human P450 antibodies in this experimental condition did not cross-react with the mouse orthologs.

Table 1
Chimeric mice used in this study.

Group	Mouse no.	Age at 1st dose (week)	hAlb concentration in the blood (mg/ml)	Approximate RI (%)
Control	1	13	9.6	80
	2	13	11.6	85
	3	13	9.1	78
	4	11	8.0	75
	5	12	9.3	79
	6	12	11.6	85
Tro 1000 mg/kg (14 days)	7	13	11.7	85
	8	13	9.6	80
	9	13	9.1	78
	10	14	9.7	80
	11	13	9.6	80
Tro 250 mg/kg (28 days)	S1	12	9.3	79
	S2	12	8.4	76
	S3	12	10.5	82
	S4	12	9.0	78
	S5	12	10.6	83
Tro 500 mg/kg (28 days)	S6	12	9.7	80
	S7	12	9.6	80
	S8	11	9.1	78
	S9	12	8.2	75
	S10	15	9.5	80
Tro 1000 mg/kg (23 days)	12	15	14.9	92
	13	14	12.3	87
	14	14	14.6	92
	15	15	8.3	76
BSO (14 days)	16	13	10.3	82
	17	13	9.2	79
	18	13	11.6	85
BSO + Tro 1000 mg/kg (14 days)	19	13	8.7	77
	20	13	10.3	82
	21	13	9.2	79

RI, replacement index.

Table 2
Sequence of primers for real-time RT-PCR analyses.

Primer	Sequence
CYP2C8 S[a]	5′-AGATCAGAATTTCTCACCC-3′
CYP2C8 AS[a]	5′-AACTTCGTGTAAGAGCAACA-3′
CYP3A4 S[a]	5′-CCAAGCTATGCTCTTCACCG-3′
CYP3A4 AS[a]	5′-TCAGGTCCACTTACGGTGC-3′
SULT1A1 S	5′-ATGGAGACTCTGAAAGACACACCGG-3′
SULT1A1 AS	5′-TGTGCTGAACCACGAAGTCCACG-3′
UGT1A1 S[b]	5′-CCTTGCCTCAGAATTCCTTC-3′
UGT1A1 AS[b]	5′-ATTGATCCCAAAGAGAAAACCAC-3′
GAPDH S[a]	5′-CCAGGGCTTTTAACTC-3′
GAPDH AS[a]	5′-GCTCCCCCCTGCAAATGA-3′

S, sense primer; AS, antisense primer.
[a] From Katoh et al. (2004).
[b] From Izukawa et al. (2009).

2.10. CYP2C8 and CYP3A4 activities

Liver microsomes from the chimeric or control mice were prepared as described previously (Katoh et al., 2004) and stored at −80 °C until analysis. The protein concentration was determined using Bradford assay reagent (Bio-Rad, Hercules, CA) with bovine γ globulin as the standard. The typical incubation mixtures (total volume, 0.2 ml) consisted of microsomes in 100 mM potassium phosphate buffer (pH 7.4) containing an NADPH-generating system (0.5 mM $NADP^+$, 5 mM glucose 6-phosphate, 5 mM $MgCl_2$, and 1 unit/ml glucose-6-phosphate dehydrogenase) and a substrate.

Paclitaxel 6α-hydroxylase activity was determined by the method of Willey et al. (1993), with slight modifications. The concentrations of the microsomes and paclitaxel were 0.5 mg/ml and 20 μM, respectively. The reaction mixture was incubated at 37 °C for 10 min, and terminated by adding 1.0 ml of dichloromethane. Testosterone (10 μl of 100 μM) was added as an internal standard. After centrifugation at 900 × *g* for 10 min, the organic phase (500 μl) was evaporated under a gentle stream of nitrogen at 40 °C. The residue was redissolved in 200 μl of mobile phase and then 100-μl portion of the sample was subjected to high-performance liquid chromatography (HPLC). The product formation was determined with a Mightysil RP-8 C8 GP column (5-μm particle size, 4.6 i.d. × 150 mm; Kanto Chemical, Tokyo, Japan). The mobile phase (45% acetonitrile/20 mM ammonium acetate) was used under isocratic condition. The flow rate was 1.0 ml/min, and the column temperature was 35 °C. The eluent was monitored at 227 nm. The quantification of 6α-hydroxypaclitaxel was performed by comparing the HPLC peak heights to that of authentic standards with reference to an internal standard. The retention time of 6α-hydroxypaclitaxel and paclitaxel was 9.0 and 14.7 min, respectively.

The dexamethasone 6-hydroxylase activity was determined according to the method of Tomlinson et al. (1997), with slight modifications. The concentrations of microsomes and dexamethasone were 1.0 mg/ml and 100 μM, respectively. The reaction mixture (total volume, 0.2 ml) was incubated at 37 °C for 30 min, and terminated by adding 1.5 ml of ice-cold ethyl acetate. 6-Hydroxytestosterone (10 μl of 10 ng/μl) was added as an internal standard. After centrifugation at 900 × *g* for 10 min, the organic phase (500 μl) was evaporated under a gentle stream of nitrogen at 40 °C. The residue was redissolved in 200 μl of mobile phase and then 100-μl portion of the sample was subjected to HPLC. The product formation was determined with a Mightysil RP-8 C8 GP column (5-μm particle size, 4.6 i.d. × 150 mm; Kanto Chemical). The mobile phase (23% acetonitrile/0.015% formic acid) was used under isocratic condition. The flow rate was 1.0 ml/min, and the column temperature was 35 °C. The eluent was monitored at 243 nm. The dexamethasone 6-hydroxylase activity was quantified using a standard curve of dexamethasone because we could not obtain pure 6-hydroxydexamethasone. The retention time of 6-hydroxydexamethasone was confirmed using the incubation product of recombinant CYP3A4 and dexamethasone. The retention time of 6-hydroxydexamethasone and dexamethasone was 4.8 and 37.7 min respectively. The final concentration of the solvent in the incubation mixture was less than 1%.

2.11. Statistical analysis

Statistical analyses between multiple groups were performed using one-way analysis of variance (ANOVA), followed by Dunnett's *post hoc* test. Comparisons between two groups were performed using two-tailed Student's *t*-test. A value of $P < 0.05$ was considered statistically significant.

Table 3
Serum biochemical parameters in toroglitazone and/or BSO-administered chimeric mice.

Group	Mouse no.	ALT (U/l)			AST (U/l)		LDH (U/l)		T-Bil (mg/dl)		D-Bil (mg/dl)	
		Initial	Final		Final		Final		Final		Final	
Control	1	108	77		147		1366		0.8		0.1	
	2	90	56		83		2884		0.7		0.1	
	3	140	139		212		1386		0.8		0.1	
	4	87	137		152		1554		0.8		ND	
	5	88	79		126		832		0.9		ND	
	6	92	106		188		1122		0.8		ND	
	Mean ± SD	101 ± 21	99 ± 34	[1.0]	151 ± 46	[1.0]	1524 ± 712	[1.0]	0.8 ± 0.1	[1.0]	0.1 ± 0.0	[1.0]
Tro 1000 mg/kg	7	64	67		170		3600		0.9		0.1	
(14 days)	8	96	233	R	345		2520		1.5		0.4	
	9	144	218	R	283		861		1.0		0.1	
	10	79	167	R	188		1724		0.8		0.1	
	11	39	64		145		897		0.9		0.1	
	Mean ± SD	84 ± 39	150 ± 81	[1.5]	226 ± 84	[1.5]	1920 ± 1161	[1.3]	1.0 ± 0.3	[1.3]	0.2 ± 0.1	[2.0]
	R (n = 3)	106 ± 34	206 ± 35**	[2.1]	272 ± 79	[1.8]	1702 ± 830	[1.1]	1.1 ± 0.4	[1.4]	0.2 ± 0.2	[2.0]
Tro 250 mg/kg	S1	62	344	R	361		2256		0.9		ND	
(28 days)	S2	71	182		250		902		0.9		ND	
	S3	75	70		165		1498		0.7		ND	
	S4	59	146	R	186		823		0.8		ND	
	S5	80	111		130		667		0.8		ND	
	Mean ± SD	69 ± 9	171 ± 105	[1.7]	218 ± 91	[1.4]	1229 ± 655	[0.8]	0.8 ± ±0.1	[1.0]	0.1 ± 0.0	[1.0]
Tro 500 mg/kg	S6	66	108		144		779		0.7		ND	
(28 days)	S7	78	205	R	318		1126		0.7		ND	
	S8	79	48		93		531		0.6		ND	
	S9	81	91		114		487		0.7		ND	
	S10	71	171	R	170		982		0.6		ND	
	Mean ± SD	75 ± 6	125 ± 63	[1.3]	168 ± 89	[1.1]	781 ± 278	[0.5]	0.7 ± 0.1	[0.9]	0.1 ± 0.0	[1.0]
Tro 1000 mg/kg	12	79	504	R	452		1566		0.6		0.1	
(23 days)	13	70	221	R	260		1550		0.7		0.1	
	14	84	345	R	410		1274		0.7		0.1	
	15	113	97		138		729		0.7		ND	
	Mean ± SD	87 ± 19	292 ± 174	[2.9]	315 ± 144	[2.1]	1280 ± 391	[0.8]	0.7 ± 0.1	[0.9]	0.1 ± 0.0	[1.0]
	R (n = 3)	78 ± 7	357 ± 142**	[3.6]	374 ± 101**	[2.5]	1463 ± 164	[1.0]	0.7 ± 0.1	[0.9]	0.1 ± 0.0	[1.0]
BSO	16	58	51		102		1728		0.8		0.2	
(14 days)	17	65	91		131		1206		0.6		0.1	
	18	53	38		123		1504		0.7		0.1	
	Mean ± SD	59 ± 6	60 ± 28	[0.6]	119 ± 15	[0.8]	1479 ± 262	[1.0]	0.7 ± 0.1	[0.9]	0.1 ± 0.1	[1.0]
BSO + Tro	19	117	59		175		1572		0.7		0.2	
1000 mg/kg	20	55	55		105		891		0.6		ND	
(14 days)	21	76	39		144		836		0.8		0.1	
	Mean ± SD	83 ± 32	51 ± 11	[0.5]	141 ± 35	[0.9]	1100 ± 410	[0.7]	0.7 ± 0.1	[0.9]	0.2 ± 0.1	[2.0]

Each parameter except initial value was measured 24 h after the last troglitazone administration.
Differences compared to the control group were considered significant at $^{**}P < 0.01$.
ND, not detected; R, responder; score in parenthesis, ratio to the control.

3. Results

3.1. TRO caused liver injury in chimeric mice with a humanized liver

TRO was orally administered to female chimeric mice at a dose of 250 mg/kg/day for 28 days (Tro 250-28 day), 500 mg/kg/day for 28 days (Tro 500-28 day), and 1000 mg/kg/day for 14 days (Tro 1000-14 day) or 23 days (Tro 1000-23 day) in a non-fasting condition. BSO (10 mM in drinking water) was treated alone or with Tro administration for 14 days. The initial serum ALT levels ranged from 39 to 144 U/l among all animals (Table 3). The final ALT levels in the Tro 250-28 day (171 ± 105 U/l), Tro 500-28 day (125 ± 63 U/l), Tro 1000-14 day (150 ± 81 U/l) and Tro 1000-23 day (292 ± 174 U/l) groups increased by 1.7-, 1.3-, 1.5- and 2.9-fold, respectively compared to the control group (99 ± 34 U/l). Two out of five mice in both Tro 250-28 day and Tro 500-28 day groups, three out of five mice in the Tro 1000-14 day group and three out of four mice in the Tro 1000-23 day group showed increased ALT levels of more than 144 U/l, the highest initial ALT level among all mice. These mice were termed responders (R) in Table 3. The average values of ALT levels in Tro 250-28 day and Tro 500-28 day groups are a little higher than the control group, however there is no clear dose–response in these values. These results suggest that the dose level of 1000 mg/kg is required for the onset of troglitazone-induced liver injury in the chimeric mice. Therefore, we put focus on the results from 1000 mg/kg dose groups in the subsequent analyses. The final ALT levels in responders in the Tro 1000-14 day and Tro 1000-23 day groups were significantly higher than those in the control group by 2.1- and 3.6-fold, respectively (Fig. 1). For the subsequent analyses, the data from the responders (R) in Tro 1000-14 day and Tro 1000-23 day groups were compared to those in the control group.

The final AST level in the Tro 1000-23 day group was significantly higher than that in the control group by 2.5-fold. The final serum LDH, T-Bil and D-Bil levels in the Tro 1000-14 day and Tro 1000-23 day groups were unchanged compared to the control group (Table 3). The LDH, T-Bil and D-Bil levels in the Tro 1000-23 day group were lower than those in the Tro 1000-14 day group. Both in the BSO alone and BSO- and Tro-administered groups, serum ALT, AST, LDH, T-Bil and D-Bil levels were unchanged compared to the levels in the control group (Table 3 and Fig. 1).

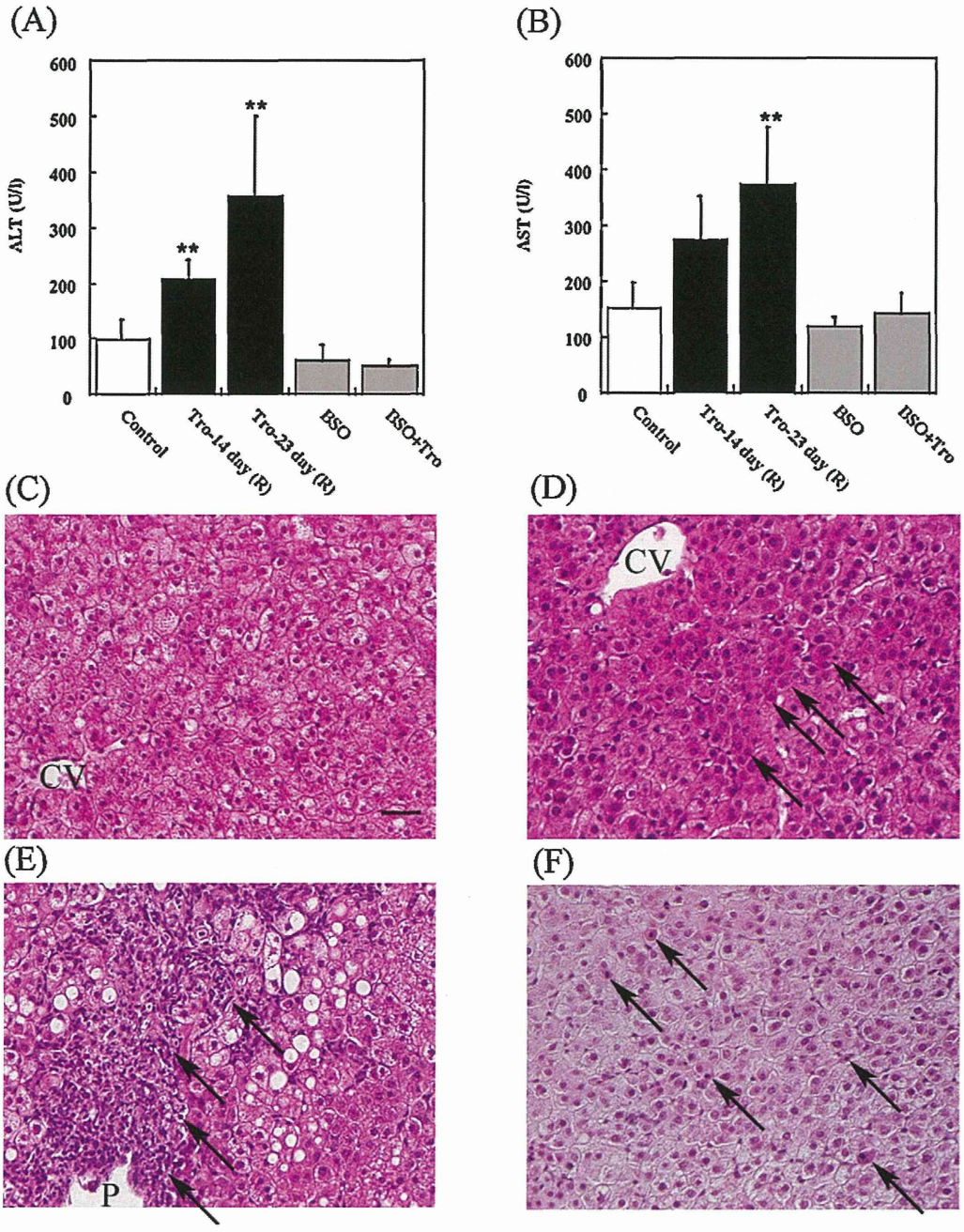

Fig. 1. Changes in the serum ALT and AST levels and liver histology by Tro and/or BSO administration in chimeric mice. The chimeric mice were orally administered Tro (1000 mg/kg/10 ml, suspended in 0.5% CMC) once daily for 14 or 23 days in a non-fasting condition, and 0.5% CMC was administered once daily for 14 days as a control. BSO (10 mM in drinking water) was also given alone or with Tro administration for 14 days. (A) ALT and (B) AST were measured 24 h after the last administration. The data are shown as the mean ± SD of the results from 3 to 6 mice. In the Tro-14 day ($n = 3$) and Tro-23 day ($n = 3$) group, the data are from the responder chimeric mice (R). The differences compared to the control group ($n = 6$) were considered significant at $^{**}P < 0.01$. (C–F) The liver specimens from the chimeric mice were sampled 24 h after the last Tro administration and subsequently stained with H&E. The human hepatocytes in the control chimeric mouse had a clear cytoplasm and no cellular infiltration (C, mouse no. 2). The arrows indicate an eosinophilic change of human hepatocytes (D, mouse no. 12, Responder), neutrophil infiltration (E, mouse no. 13, Responder) and necrosis of human hepatocytes (F, mouse no. 14, Responder). CV: central vein; P: portal vein; Bars: 40 μm (C–F are the same scale).

In the control chimeric mouse, a clear cytoplasm and no cellular infiltration were observed in the human hepatocytes in the liver tissue of the chimeric mice (Fig. 1C). In the responder chimeric mice, the human hepatocytes in the liver tissue showed slight eosinophilic changes (Fig. 1D), neutrophil infiltration surrounding the area of the portal vein (Fig. 1E) and scattered single cell necrosis (Fig. 1F) after Tro administration.

3.2. Oxidative stress responses in chimeric mice with a humanized liver

In both the Tro 1000-14 day and Tro 1000-23 day groups, the hepatic GSH contents were significantly higher in the Tro-administered responder mice by approximately 2-fold than in the control group (Fig. 2A). GST activities, SOD2 activities and the

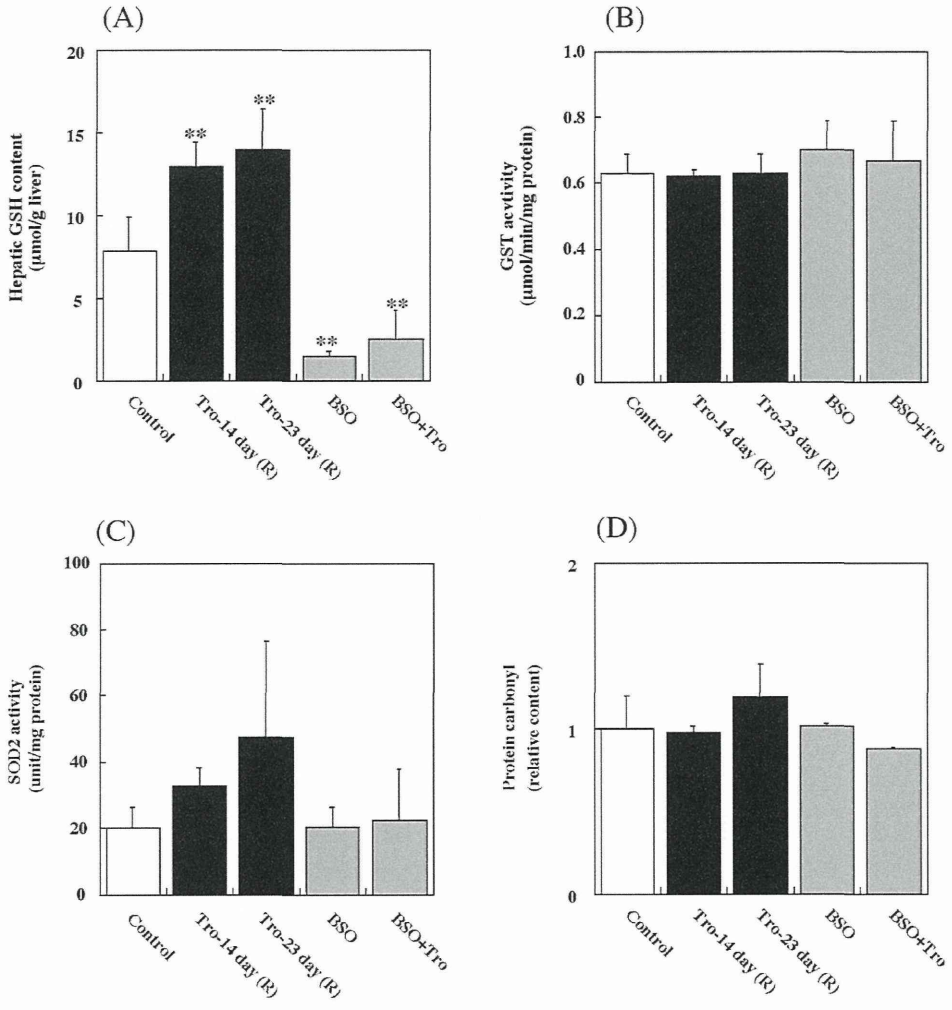

Fig. 2. Changes in the hepatic GSH content (A), GST activity (B), SOD2 activity (C), and plasma protein carbonyl content (D) in the chimeric mice that were administered Tro and/or BSO. The data are shown as the mean ± SD of the results from 3 to 6 mice. In the Tro-14 day and Tro-23 day groups, the data are from the responder chimeric mice. The differences compared to the control group were considered significant at $^{**}P < 0.01$.

protein carbonyl content showed no significant change following Tro administration (Fig. 2B–D). SOD2 activity in the Tro 1000-23 day group was higher than in the control: however, the difference in activity was not significant.

The effects of the GSH-lowering agent BSO on oxidative stress in the chimeric mice were evaluated. The hepatic GSH contents were significantly decreased in the BSO group by approximately 0.2-fold compared to the control group. However, in the BSO and Tro-administered group, the GSH content was suppressed by Tro administration. The hepatic GST activities were unchanged with the administration of BSO alone or BSO and Tro administration. The administration of BSO and Tro showed no change in SOD2 activity. The protein carbonyl contents also showed no change among the groups in this study (Fig. 2D). These results suggested that Tro induced the GSH synthesis enzyme, which was inhibited by BSO.

3.3. *Effect of Tro and/or BSO administration on the expression of drug metabolizing enzymes in the chimeric mice with a humanized liver*

We determined the expression levels of drug metabolizing enzymes, which are involved in the metabolism of Tro in human. The expression level of human CYP2C8 mRNA (Fig. 3A) was increased with the administration of Tro and/or BSO. The expression level of CYP2C8 protein (Fig. 3B) and paclitaxel 6a-hydroxylase activities (Fig. 3C) were significantly increased by the administration of Tro. The expression levels of CYP3A4 mRNA (Fig. 4A) and protein (Fig. 4B) also tended to increase with the administration of Tro and/or BSO. Dexamethasone 6-hydroxylase activities were significantly increased by the administration of Tro and/or BSO. Therefore, these results clearly demonstrated that Tro induced CYP2C8 and CYP3A4 in the liver of the chimeric mice with a humanized liver. Interestingly, the administration of BSO alone also induced both enzymes. Based on these data, enzyme induction is unlikely to be involved in Tro-induced liver injury. In addition, we found that Tro induced the expression level of human UGT1A1 (Fig. 5B) mRNA. The administration of BSO and/or Tro also induced the expression level of UGT1A1 mRNA.

4. Discussion

During the preclinical development and following the withdrawal of Tro, pharmaceutical companies performed numerous toxicity studies using mice, rats and monkeys (Watanabe et al.,

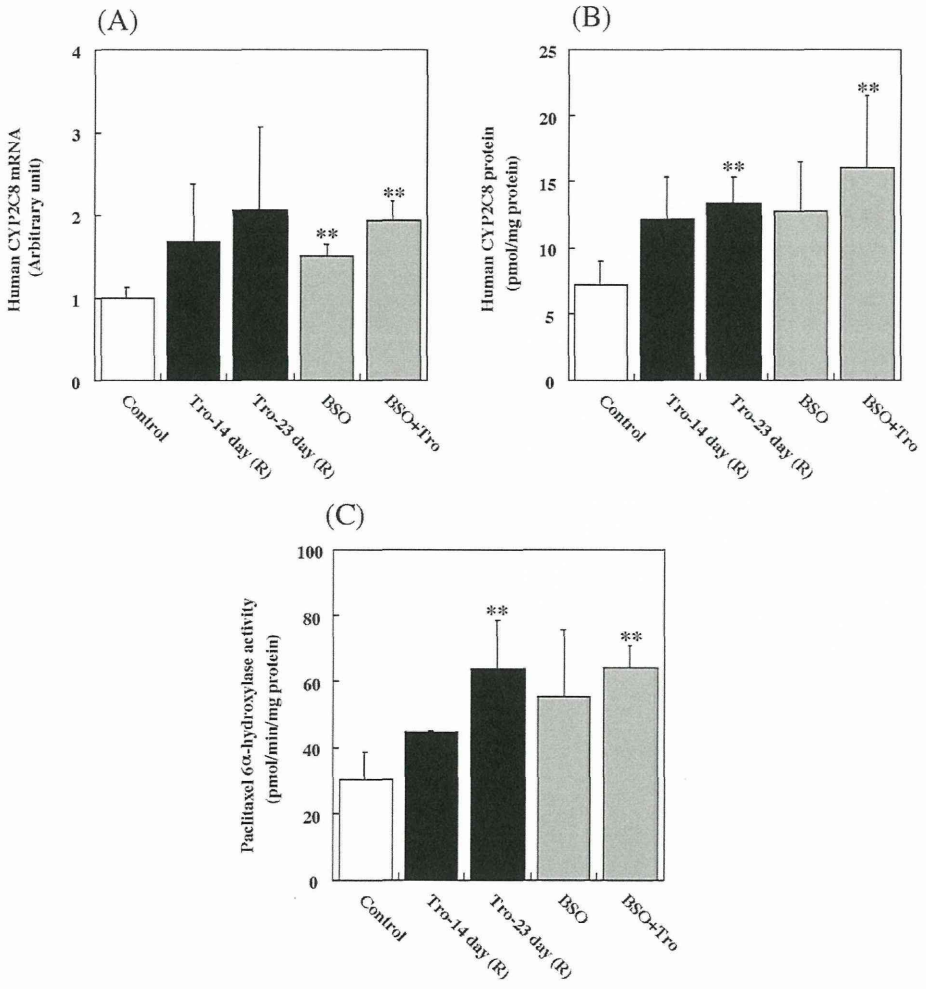

Fig. 3. Changes in the expression level of human CYP2C8 mRNA (A), protein content (B), and enzyme activity (C) in the liver of chimeric mice that were administered Tro and/or BSO. Paclitaxel 6a-hydroxylase activity was catalyzed by CYP2C8 and measured using 20 μM paclitaxel as a substrate. The data are shown as the mean ± SD of the results from 3 to 6 mice. In the Tro-14 day and Tro-23 day groups, the data are from the responder chimeric mice. The differences compared to the control group were considered significant at $^{**}P < 0.01$.

1999). In these toxicity studies, Tro was administered at a dose of 800 mg/kg/day for 24 months to mice, 1200 mg/kg/day for 12 months to rats and 1200 mg/kg/day for 12 months to monkeys, but no signs of liver dysfunction were confirmed (Watanabe et al., 1999). Chimeric mice with a humanized liver are suitable for *in vivo* studies utilizing human hepatocytes. The present study used chimeric mice with a humanized liver and successfully demonstrated Tro-induced liver with the once daily oral administration for 14 and 23 days of 1000 mg/kg Tro. The development of Tro-induced liver injuries in the responder chimeric mice was confirmed by the significant increase in the final serum ALT and AST levels that occurred in an administration-duration-dependent manner (Fig. 1A and B), the eosinophilic changes (Fig. 1D) and cellular infiltrations in the liver tissue (Fig. 1E) and single cell necrosis of human hepatocytes (Fig. 1F). Using the same chimeric mice, Schulz-Utermoehl et al. (2012) did not demonstrate liver injury administering a once daily oral dose for 7 days of 300 and 600 mg/kg Tro, and no significant differences in the pharmacokinetics parameters of C_{max} or AUC were observed following doses of Tro at 300 and 600 mg/kg. These evidences support our results that 250 and 500 mg/kg of Tro was insufficient for the onset of Tro-induced liver injury in the chimeric mice when dosed once daily for 28 days. Both the dose level and the dosing period will be essential factors for the onset of Tro-induced liver injury.

The increase of serum transaminases was considered to be derived from the human hepatocytes, which was supported by the histological changes. However, we were unable to distinguish human ALT from mouse ALT quantitatively (data not shown). Conversely, two out of five mice in the Tro 1000-14 day group and one out of four mice in the Tro 1000-23 day group did not show hepatic injury. As shown in Table 1, the chimeric mice exhibited a hAlb concentration of 8.0–14.9 mg/ml and 75–92% of RI and received transplanted human hepatocytes from the same donor. The hAlb levels of the non-responder chimeric mice ranged from 8.2 (RI: 75%) to 11.7 mg/ml (RI; 85%), and appeared to not be critically different from the hAlb levels of the responder chimeric mice, which ranged from 9.0 (RI: 78%) to 14.9 (RI: 92%). Therefore, it was considered that the individual difference in the onset of liver injury among the mice would depend on other factors as discussed below.

It has been reported that the double null mutant of GSTT1 and GSTM1 in humans correlated with Tro-associated abnormal increases in ALT levels (odds ratio, 3.692; 95% confidence interval, 1.354–10.066; $P = 0.008$) (I. Watanabe et al., 2003). However, the present study revealed that the difference in the onset of liver injury

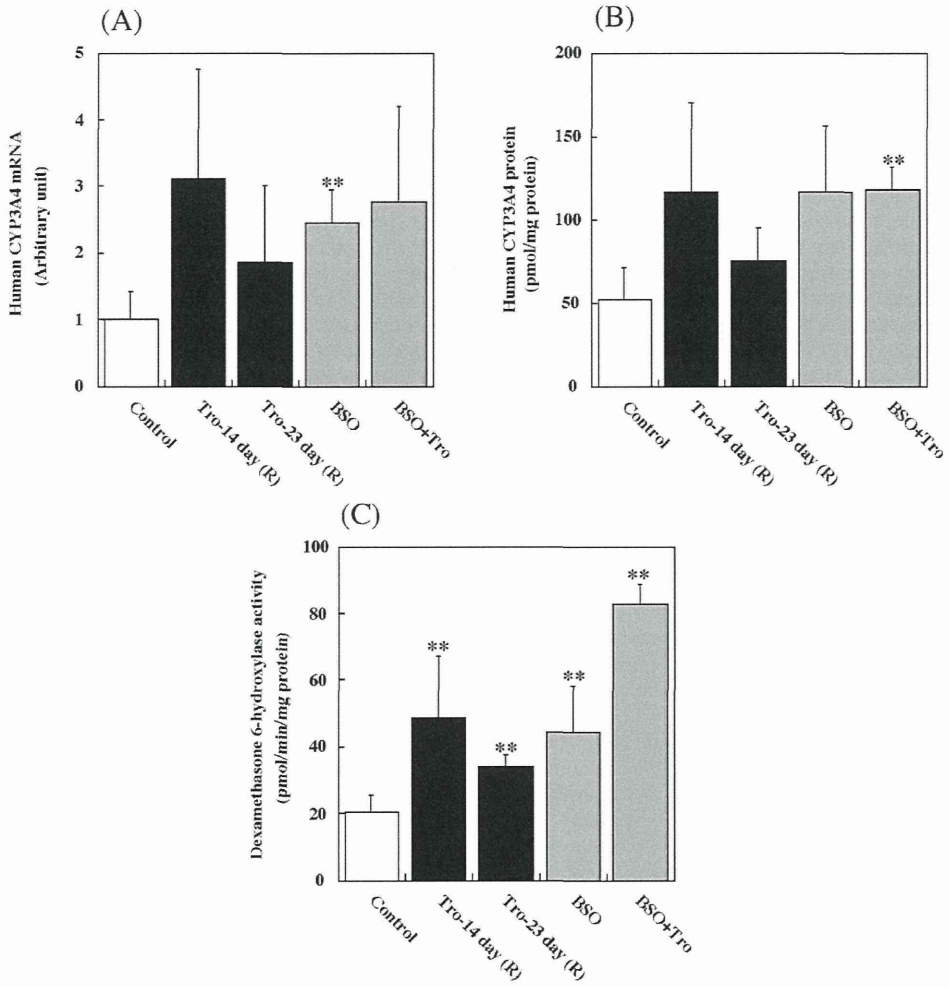

Fig. 4. Changes in the expression level of human CYP3A4 mRNA (A), protein content (B), and enzyme activity (C) in the liver of chimeric mice administered Tro and/or BSO. Dexamethasone 6-hydroxylase activity was catalyzed by CYP3A4 and measured using 100 μM dexamethasone as a substrate. The data are shown as the mean ± SD of the results from 3 to 6 mice. In the Tro-14 day and Tro-23 day groups, the data are from the responder chimeric mice. The differences compared to the control group were considered significant at $^{**}P < 0.01$.

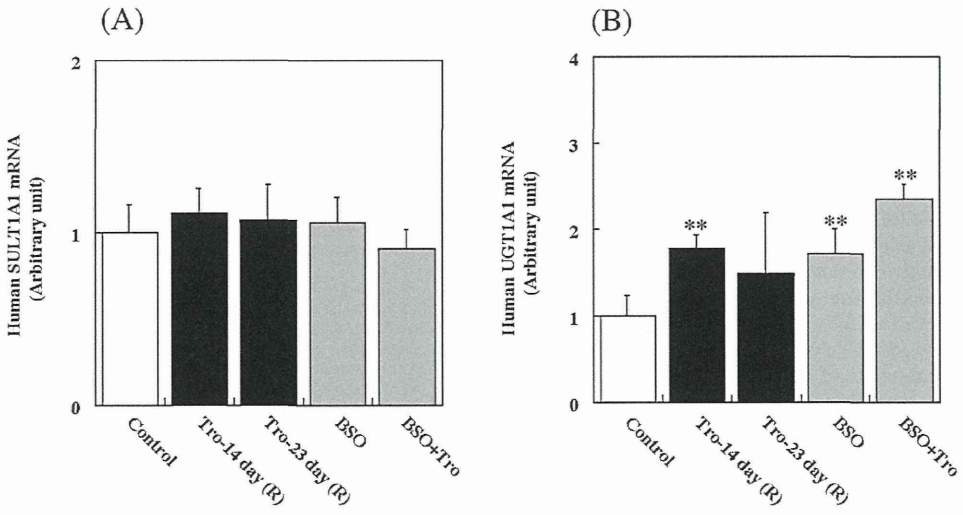

Fig. 5. Changes in the expression level of human SULT1A1 mRNA (A) and human UGT1A1 mRNA expression (B) in the liver of chimeric mice that were administered Tro and/or BSO. The data are shown as the mean ± SD of the results from 3 to 6 mice. In the Tro-14 day and Tro-23 day groups, the data are from the responder chimeric mice. The differences compared to the control group were considered significant at $^{**}P < 0.01$.

could be Tro-induced in the chimeric mice with genetically identical human hepatocytes genotyped to wild-type GSTT1 and GSTM1 (data not shown). It is conceivable that the double null mutant of GSTT1 and GSTM1 is unlikely to be a risk factor, which was recently suggested by Usui et al. (2011) using cytotoxicity assays of human hepatocytes.

BSO was administered to evaluate the effects of GSH depletion on Tro-induced liver injury. The suspected active metabolite of Tro, a quinone metabolite, has been reported to not react directly with GSH, and it can be further metabolized to an *O*-quinone methide or undergo ring opening to produce additional highly electrophilic intermediates (Kassahun et al., 2001). However, in this study, neither the serum biochemical analyses nor the histological examinations showed evidence of liver injury in the BSO alone and BSO- and Tro-administered group, whereas the hepatic GSH contents decreased approximately 0.2- and 0.4-fold in these groups, respectively compared to the control group (Fig. 2A). Furthermore, hepatic GST activities were maintained in all groups (Fig. 2B). Although the results in this study appear to not support the general understanding of scavenging systems for reactive metabolites, it was suggested that the onset of Tro-induced liver injury was independent of scavenging systems associated with hepatic GSH. Interestingly, the hepatic GSH contents significantly increased with the administration of Tro (Fig. 2A), although the functional mechanism in relation to the onset of liver injury was unclear.

SOD2 activity and protein carbonyl contents were measured to clarify whether an increase in oxidative stress might be associated with the onset of Tro-induced liver injury (Fig. 2C and D), as reported in a study using *SOD2*$^{+/-}$ mice (Ong et al., 2007). In the *SOD2*$^{+/-}$ mouse study, the increase in the serum AST level and the degeneration of hepatocytes were observed when 30 mg/kg of Tro was intraperitoneally administered once per day for 4 weeks (Ong et al., 2007). However, the phenomenon was not reproduced by other group (Fujimoto et al., 2009) despite the administered to the same dose to the same *SOD2*$^{+/-}$ mice. We found that SOD2 activities were tended to increase in the Tro-23 day group. Furthermore, the protein carbonyl contents were unchanged. These results suggest that oxidative stress may not involved in Tro-induced liver injury in the chimeric mice.

In humans, Tro is metabolized by three pathways, *i.e.*, sulfation by SULT1A1 (Honma et al., 2002), glucuronidation by UGT1A1 (Yoshigae et al., 2000), and oxidation to form a quinone metabolite (M3) by CYP2C8 and CYP3A4 (Yamazaki et al., 1999; Yamamoto et al., 2002). Recently, the chimeric mice were confirmed to show the unique profiles in metabolism of Tro when compared to SCID mice (Schulz-Utermoehl et al., 2012). A total of 32 putative metabolites plus Tro were detected in blood from the chimeric mice, with 14 (M1, M4–M10, M12 and M17–M21) of these metabolites detected only in blood from the chimeric mice. Of these 14 metabolites, 4 (M4, M7, M8 and M12) were also detected only in liver extracts from the chimeric mice. The relative concentrations of the glucuronide metabolite (M13) were higher in liver preparations from SCID mice. These findings suggested the chimeric mice possess metabolically active human hepatocytes and have a potential to generate unique human metabolite (Schulz-Utermoehl et al., 2012). The involvement of a sulfo-conjugate in Tro-induced liver injury was suggested in *in vitro* study by Saha et al. (2010) who reported that a sulfo-conjugate of Tro exerted direct toxic effects on human hepatocytes, possibly *via* oxidative stress induction. In contract, the expression level of SULT1A1 mRNA was not changed in this study, suggesting the difference effect of Tro between *in vivo* and *in vitro* study.

We found that CYP2C8 and CYP3A4 were induced by the administration of Tro, as previously reported (Sahi et al., 2003). However, the onset of the Tro-induced liver injury was considered independent of the induction of these drug-metabolizing enzymes because enzyme induction was also observed in the BSO alone- and BSO and Tro-administered group. The cause of the moderate induction of CYP3A4 in the Tro-23 day group compared with the Tro-14 day group remains unclear. However, it was reported that hepatic expression levels of proinflammatory cytokines, tumor necrosis factor (TNF) α and interleukin (IL)-6 and chemokines were increased in the mouse model of drug-induced liver injury (Toyoda et al., 2011, 2012). TNFα was also identified to be involved in the down-regulation of CYP3A11 and CYP3A25 in mouse liver (Kinloch et al., 2011). In addition, IL-6 was reported to down-regulate the expression of CYP3A4 *via* pregnane X receptor in human hepatocytes (Yang et al., 2010). Taking these recent reports into consideration, chronic hepatic inflammation in the Tro-23 day group might be a causal factor for the decreased expression level of CYP3A4 in this study.

As shown in Fig. 5B, UGT1A1 appears unrelated to the onset of the Tro-induced liver injury because significant increases in human UGT1A1 mRNA expression were observed not only in the Tro-14 day group but also in the BSO alone and BSO- and Tro-administered groups.

Notably, the chimeric mice were generated using an uPA$^{+/+}$/SCID mouse line, which is defective in functional T and B lymphocytes (Bosma et al., 1983). Tro-induced liver injury in the chimeric mice could be successfully produced when free from T and B lymphocyte-mediated immune responses. However, SCID mice were once daily orally administered Tro at 300 and 600 mg/kg doses for 7 days and showed no change in ALT and AST levels (Schulz-Utermoehl et al., 2012). Further investigations comparing SCID mice and the chimeric mice with a humanized liver are necessary.

Idiosyncratic liver injury is a critical issue for clinical practice and drug development. Thus, numerous attempts have been made to establish a method for predicting idiosyncratic liver injury in human. The present study succeeded in demonstrating Tro-induced liver injury using chimeric mice with a humanized liver. The advantage of this mouse model is to enable human hepatocytes to be examined in an *in vivo* environment. The chimeric mice with a humanized liver will be a useful tool to investigate the unsolved mechanism of idiosyncratic Tro-induced hepatic injury.

Funding information

Health and Labor Sciences Research Grants from the Ministry of Health, Labor, and Welfare of Japan (H23-BIO-G001).

Conflict of interest statement

The authors declare that there are no conflicts of interest.

References

Bedoucha, M., Atzpodien, E., Boelsterli, U.A., 2001. Diabetic KKAy mice exhibit increased hepatic PPARγ1 gene expression and develop hepatic steatosis upon chronic treatment with antidiabetic thiazolidinediones. Journal of Hepatology 35, 17–23.

Bosma, G.C., Custer, R.P., Bosma, M.J., 1983. A severe combined immunodeficiency mutation in the mouse. Nature 301, 527–530.

Fujimoto, K., Kumagai, K., Ito, K., Arakawa, S., Ando, Y., Oda, S., Yamoto, T., Manabe, S., 2009. Sensitivity of liver injury in heterozygous Sod2 knockout mice treated with troglitazone or acetaminophen. Toxicologic Pathology 37, 193–200.

Habig, W.H., Pabst, M.J., Jakoby, W.B., 1974. Glutathione S-transferases. The first enzymatic step in mercapturic acid formation. Journal of Biological Chemistry 249, 7130–7139.

He, K., Talaat, R.E., Pool, W.F., Reily, M.D., Reed, J.E., Bridges, A.J., Woolf, T.F., 2004. Metabolic activation of troglitazone: identification of a reactive metabolite and mechanisms involved. Drug Metabolism and Disposition: The Biological Fate of Chemicals 32, 639–646.

Honma, W., Shimada, M., Sasano, H., Ozawa, S., Miyata, M., Nagata, K., Ikeda, T., Yamazoe, Y., 2002. Phenol sulfotransferase, ST1A3, as the main enzyme catalyzing sulfation of troglitazone in human liver. Drug Metabolism and Disposition: The Biological Fate of Chemicals 30, 944–949.

Izukawa, T., Nakajima, M., Fujiwara, R., Yamanaka, H., Fukami, T., Takamiya, M., Aoki, Y., Ikushiro, S., Sakaki, T., Yokoi, T., 2009. Quantitative analysis of UDP-glucuronosyltransferase (UGT) 1A and UGT2B expression levels in human livers. Drug Metabolism and Disposition: The Biological Fate of Chemicals 37, 1759–1768.

Jia, D.M., Tabaru, A., Akiyama, T., Abe, S., Otsuki, M., 2000. Troglitazone prevents fatty changes of the liver in obese diabetic rats. Journal of Gastroenterology and Hepatology 15, 1183–1191.

Kassahun, K., Pearson, P.G., Tang, W., McIntosh, I., Leung, K., Elmore, C., Dean, D., Wang, R., Doss, G., Baillie, T.A., 2001. Studies on the metabolism of troglitazone to reactive intermediates in vitro and in vivo. Evidence for novel biotransformation pathways involving quinone methide formation and thiazolidinedione ring scission. Chemical Research in Toxicology 14, 62–70.

Katoh, M., Matsui, T., Nakajima, M., Tateno, C., Kataoka, M., Soeno, Y., Horie, T., Iwasaki, K., Yoshizato, K., Yokoi, T., 2004. Expression of human cytochromes P450 in chimeric mice with humanized liver. Drug Metabolism and Disposition: The Biological Fate of Chemicals 32, 1402–1410.

Katoh, M., Matsui, T., Okumura, H., Nakajima, M., Nishimura, M., Naito, S., Tateno, C., Yoshizato, K., Yokoi, T., 2005. Expression of human phase II enzymes in chimeric mice with humanized liver. Drug Metabolism and Disposition: The Biological Fate of Chemicals 33, 1333–1340.

Katoh, M., Sawada, T., Soeno, Y., Nakajima, M., Tateno, C., Yoshizato, K., Yokoi, T., 2007. In vivo drug metabolism model for human cytochrome P450 enzyme using chimeric mice with humanized liver. Journal of Pharmaceutical Sciences 96, 428–437.

Kinloch, R.D., Lee, C.M., van Rooijen, N., Morgan, E.T., 2011. Selective role for tumor necrosis factor-α, but not interleukin-1 or Kupffer cells, in down-regulation of CYP3A11 and CYP3A25 in livers of mice infected with a noninvasive intestinal pathogen. Biochemical Pharmacology 82, 312–321.

Nishimura, M., Yoshitsugu, H., Yokoi, T., Tateno, C., Kataoka, M., Horie, T., Yoshizato, K., Naito, S., 2005. Evaluation of mRNA expression of human drug-metabolizing enzymes and transporters in chimeric mouse with humanized liver. Xenobiotica 35, 877–890.

Ong, M.M., Latchoumycandane, C., Boelsterli, U.A., 2007. Troglitazone-induced hepatic necrosis in an animal model of silent genetic mitochondrial abnormalities. Toxicological Sciences 97, 205–213.

Saha, S., New, L.S., Ho, H.K., Chui, W.K., Chan, E.C.Y., 2010. Direct toxicity effects of sulfo-conjugated troglitazone on human hepatocytes. Toxicology Letters 195, 135–141.

Sahi, J., Black, C.B., Hamilton, G.A., Zheng, X., Jolley, S., Rose, K.A., Gilbert, D., LeCluyse, E.L., Sinz, M.W., 2003. Comparative effects of thiazolidinediones on in vitro P450 enzyme induction and inhibition. Drug Metabolism and Disposition: The Biological Fate of Chemicals 31, 439–446.

Schulz-Utermoehl, T., Sarda, S., Foster, J.R., Jacobsen, M., Kenna, J.G., Morikawa, Y., Salmu, J., Gross, G., Wilson, I.D., 2012. Evaluation of the pahrmacokinetics, biotransformation, and hepatic transporter effects of troglitazone in mice with humanized livers. Xenobiotica 42, 503–517.

Tateno, C., Yoshizane, Y., Saito, N., Kataoka, M., Utoh, R., Yamasaki, C., Tachibana, A., Soeno, Y., Asahina, K., Hino, H., Asahara, T., Yokoi, T., Furukawa, T., Yoshizato, K., 2004. Near completely humanized liver in mice shows human-type metabolic responses to drugs. American Journal of Pathology 165, 901–912.

Tettey, J.N., Maggs, J.L., Rapeport, W.G., Pirmohamed, M., Park, B.K., 2001. Enzyme induction dependent bioactivation of troglitazone and troglitazone quinone in vivo. Chemical Research in Toxicology 14, 965–974.

Tietze, F., 1969. Enzymatic method for quantitative determination of nanogram amounts of total and oxidized glutathione: applications to mammalian blood and other tissues. Analytical Biochemistry 27, 502–522.

Tomlinson, E.S., Maggs, J.L., Park, B.K., Back, D.J., 1997. Dexamethasone metabolism in vitro: species differences. Journal of Steroid Biochemistry and Molecular Biology 62, 345–352.

Toyoda, Y., Miyashita, T., Endo, S., Tsuneyama, K., Fukami, T., Nakajima, M., Yokoi, T., 2011. Estradiol and progesterone modulate halothane-induced liver injury in mice. Toxicology Letters 204, 17–24.

Toyoda, Y., Endo, S., Tsuneyama, K., Miyashita, T., Yano, A., Fukami, T., Nakajima, M., Yokoi, T., 2012. Mechanism of exacerbative effect of progesterone on drug-induced liver injury. Toxicological Sciences 126, 16–27.

Usui, T., Hashizume, T., Katumata, T., Yokoi, T., Komuro, S., 2011. In vitro investigation of the glutathione transferase M1 and T1 null genotypes as risk factors for troglitazone-induced liver injury. Drug Metabolism and Disposition: The Biological Fate of Chemicals 39, 1303–1310.

Watanabe, T., Ohashi, Y., Yasuda, M., Takaoka, M., Furukawa, T., Yamoto, T., Sanbuissho, A., Manabe, S., 1999. Was it not possible to predict liver dysfunction caused by troglitazone during the nonclinical safety studies? Reevaluation of Safety 30, 537–546.

Watanabe, T., Furukawa, T., Sharyo, S., Ohashi, Y., Yasuda, M., Takaoka, M., Manabe, S., 2000. Effect of troglitazone on the liver of a Gunn rat model of genetic enzyme polymorphism. Journal of Toxicological Sciences 25, 423–431.

Watanabe, I., Tomita, A., Shimizu, M., Sugawara, M., Yasumo, H., Koishi, R., Takahashi, T., Miyoshi, K., Nakamura, K., Izumi, T., Matusshita, Y., Furukawa, H., Haruyama, H., Koga, T., 2003. A study to survey susceptible genetic factors responsible for troglitazone-associated hepatotoxicity in Japanese patients with type 2 diabetes mellitus. Clinical Pharmacology and Therapeutics 73, 435–455.

Watanabe, T., Sagisaka, H., Arakawa, S., Shibaya, Y., Watanabe, M., Igarashi, I., Tanaka, K., Totsuka, S., Takasaki, W., Manabe, S., 2003. A novel model of continuous depletion of glutathione in mice treated with L-buthionine (S, R)-sulfoximine. Journal of Toxicological Sciences 28, 455–469.

Willey, T.A., Bekos, E.J., Gaver, R.C., Duncan, G.F., Tay, L.K., Beijnen, J.H., Farmen, R.H., 1993. High-performance liquid chromatographic procedure for the quantitative determination of paclitaxel (Taxol) in human plasma. Journal of Chromatography 621, 231–238.

Yamamoto, Y., Yamazaki, H., Ikeda, T., Watanabe, T., Iwabuchi, H., Nakajima, M., Yokoi, T., 2002. Formation of a novel quinone epoxide metabolite of troglitazone with cytotoxicity to HepG2 cells. Drug Metabolism and Disposition: The Biological Fate of Chemicals 30, 155–160.

Yamazaki, H., Shibata, A., Suzuki, M., Nakajima, M., Shimada, N., Guengerich, F.P., Yokoi, T., 1999. Oxidation of troglitazone to a quinone-type metabolite catalyzed by cytochrome P-450 2C8 and P-450 3A4 in human liver microsomes. Drug Metabolism and Disposition: The Biological Fate of Chemicals 27, 1260–1266.

Yang, J., Hao, C., Yang, D., Shi, D., Song, X., Luan, X., Hu, G., Yan, G., 2010. Pregnane X receptor is required for interleukin-6-mediated down-regulation of cytochrome P450 3A4 in human hepatocytes. Toxicology Letters 197, 219–226.

Yoshigae, Y., Konno, K., Takasaki, W., Ikeda, T., 2000. Characterization of UDP-glucuronosyltransferases (UGTs) involved in the metabolism of troglitazone in rats and humans. Journal of Toxicological Sciences 25, 433–441.

Yoshikawa, Y., Morita, M., Hosomi, H., Tsuneyama, K., Fukami, T., Nakajima, M., Yokoi, T., 2009. Knockdown of superoxide dismutase 2 enhances acetaminophen-induced hepatotoxicity in rat. Toxicology 264, 89–95.

1521-009X/12/4012-2267–2272$25.00
DRUG METABOLISM AND DISPOSITION
Vol. 40, No. 12
47555/3804647
DMD 40:2267–2272, 2012

Predictability of Metabolism of Ibuprofen and Naproxen Using Chimeric Mice with Human Hepatocytes

Seigo Sanoh, Aya Horiguchi, Kazumi Sugihara, Yaichiro Kotake, Yoshitaka Tayama, Naoto Uramaru, Hiroki Ohshita, Chise Tateno, Toru Horie, Shigeyuki Kitamura, and Shigeru Ohta

Graduate School of Biomedical and Health Sciences (S.S., A.H., Y.K., S.O.) and Liver Research Project Center (C.T.), Hiroshima University, Hiroshima, Japan; Faculty of Pharmaceutical Science, Hiroshima International University, Hiroshima, Japan (K.S., Y.T.); Nihon Pharmaceutical University, Saitama, Japan (N.U., S.K.); PXB-Mouse Production Department (H.O.) and R&D Department (C.T.), PhoenixBio Co., Ltd., Hiroshima, Japan; and DeThree Research Laboratories, Ibaraki, Japan (T.H.)

Received June 27, 2012; accepted August 30, 2012

ABSTRACT:

Prediction of human drug metabolism is important for drug development. Recently, the number of new drug candidates metabolized by not only cytochrome P450 (P450) but also non-P450 has been increasing. It is necessary to consider species differences in drug metabolism between humans and experimental animals. We examined species differences of drug metabolism, especially between humans and rats, for ibuprofen and (*S*)-naproxen as nonsteroidal anti-inflammatory drugs, which are metabolized by P450 and UDP-glucuronosyltransferase, sulfotransferase, and amino acid *N*-acyltransferase for taurine conjugation in liver, using human chimeric mice (h-PXB mice) repopulated with human hepatocytes and rat chimeric mice (r-PXB mice) transplanted with rat hepatocytes. We performed the direct comparison of excretory metabolites in urine between h-PXB mice and reported data for humans as well as between r-PXB mice and rats after administration of ibuprofen and (*S*)-naproxen. Good agreement for urinary metabolites (percentage of dose) was observed not only between humans and h-PXB mice but also between rats and r-PXB mice. Therefore, the metabolic profiles in humans and rats reflected those in h-PXB mice and r-PXB mice. Our results indicated that h-PXB mice should be helpful for predicting the quantitative metabolic profiles of drugs mediated by P450 and non-P450 in liver, and r-PXB mice should be helpful for evaluation of species differences in these metabolic enzymes.

Introduction

It is important to predict human drug metabolism and pharmacokinetics (PK) during the preclinical stage in the pharmaceutical industry because PK contributes to efficacy and toxicity, and the attrition rate during drug development has been decreasing as a result of improvement of predictability with regard to human metabolism (Kola and Landis, 2004).

The number of new drug candidates metabolized by not only cytochrome P450 (P450) but also non-P450 has been increasing, and they show diverse chemical structures, including a carboxyl group to avoid metabolism by P450. Various approaches to predict human metabolism and PK using an in vitro metabolic system with human liver microsomes, S9 fraction, and hepatocytes have been reported (Obach et al., 1997; Nagilla et al., 2006; Brown et al., 2007; Fagerholm, 2007; Stringer et al., 2008; Anderson et al., 2009; Chiba et al., 2009; Dalvie et al., 2009; Hallifax et al., 2010). However, these methods have some limits for prediction. The above reports indicated that it was difficult to predict secondary metabolism owing to the complication of multiple drug metabolic enzymes such as P450 and non-P450 because the success rate corresponding to the observed metabolites using hepatocytes was low (Anderson et al., 2009; Dalvie et al., 2009).

Chimeric mice with humanized liver, generated using urokinase-type plasminogen activator [uPA(+/+)]/severe combined immunodeficiency (SCID) mice (h-PXB mice) repopulated with human hepatocytes (PhoenixBio Co., Ltd., Hiroshima, Japan) have been reported (Tateno et al., 2004). These mice are transplanted with approximately 80% of human hepatocytes, and the expression levels and activities of P450 and non-P450 in the liver of h-PXB mice are similar to those of humans (Katoh et al., 2004, 2005; Nishimura et al., 2005; Katoh and Yokoi, 2007; Kitamura et al., 2008).

Some specific metabolites were qualitatively detected in the urine and plasma of h-PXB mice (Inoue et al., 2009; Yamazaki et al., 2010; De Serres et al., 2011; Sanoh et al., 2012b). Thus, h-PXB mice could be a good in vivo model for predicting drug metabolism in humans. However, previous investigations for quantitative prediction as well as qualitative prediction of human metabolites involved in multiple metabolic pathways from data in h-PXB mice have been insufficient.

This work was supported by the Japan Society for the Promotion of Science [Grant-in-Aid for Young Scientists (B) 22790109] and PhoenixBio, Co., Ltd.

Article, publication date, and citation information can be found at http://dmd.aspetjournals.org.

http://dx.doi.org/10.1124/dmd.112.047555.

ABBREVIATIONS: PK, pharmacokinetics; P450, cytochrome P450; SCID, severe combined immunodeficiency; h-PXB mice, human chimeric mice; UGT, UDP-glucuronosyltransferase; SULT, sulfotransferase; r-PXB mice, rat chimeric mice; RI, replacement index; LC, liquid chromatography; MS/MS, tandem mass spectrometry.

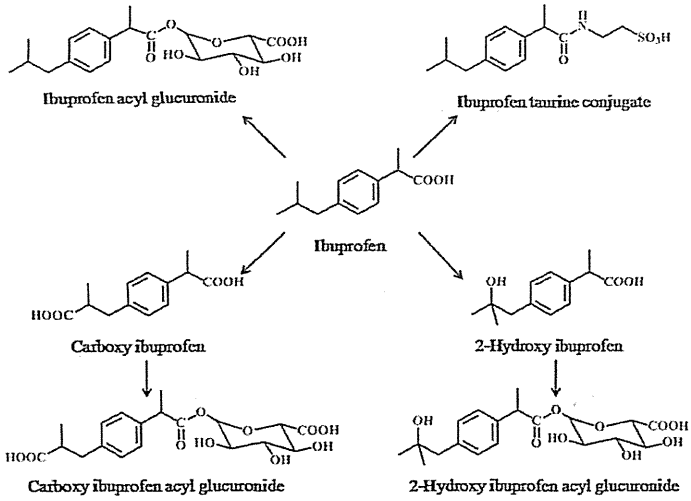

FIG. 1. Proposed metabolic pathways of ibuprofen in humans. This figure was drawn from the data of Shirley et al. (1994) and Kepp et al. (1997).

Racemic ibuprofen and (*S*)-naproxen have been widely used as nonsteroidal anti-inflammatory drugs, which are metabolized by certain metabolic enzymes such as P450 and UDP-glucuronosyltransferase (UGT), sulfotransferase (SULT), and amino acid *N*-acyltransferase for taurine conjugation in liver (Figs. 1 and 2). These metabolites are mainly excreted in urine. Furthermore, species differences in the metabolism of ibuprofen and (*S*)-naproxen between rats and humans have also been reported (Mills et al., 1973; Sugawara et al., 1978).

In this study, rat chimeric mice (r-PXB mice) containing rat hepatocytes were used to compare the metabolism and PK between rats and humans, as well as h-PXB mice, as an in vivo approach (Tateno et al., 2004; Emoto et al., 2005; Yamazaki et al., 2010; Sanoh et al., 2012b). The aim of this study was to assess the quantitative predictability of the metabolism by P450 and non-P450 by examining urinary excreted metabolites in h-PXB mice and r-PXB mice after administration of ibuprofen and (*S*)-naproxen.

Materials and Methods

Chemicals. 2-(4-Isobutylphenyl)-propionic acid (ibuprofen) and 2-(3-benzoylphenyl)-propionic acid (ketoprofen) were purchased from Wako Pure Chemicals (Osaka, Japan). (*S*)-(+)-2-(6-Methoxy-2-naphthyl)propionic acid [(*S*)-naproxen] was purchased from Cayman Chemical (Ann Arbor, Michigan). 2-[4-(2-Carboxypropyl)phenyl]-propionic acid (carboxy ibuprofen), 2-[4-(2-hydroxy-2-methylpropyl) phenyl]-propionic acid (2-hydroxylibuprofen), (*S*)-(+)-2-(6-hydroxy-2-naphthyl)-propionic acid [(*S*)-*O*-desmethylnaproxen], and (*S*)-naproxen acyl-β-D-glucuronide were obtained from Toronto Research Chemicals, Inc. (North York, ON, Canada). Ibuprofen taurine conjugate was synthesized in accordance with Shirley et al. (1994). All of the other reagents and solvents were commercial products of the highest available grade or analytical grade.

Animals. The present study was approved by the animal ethics committee and was conducted in accordance with the regulations on the use of living modified organisms of Hiroshima University. Sprague-Dawley rats (6 weeks of age) and SCID mice (10 weeks of age) were purchased from Charles River Laboratories Japan, Inc. (Yokohama, Japan). h-PXB mice and r-PXB mice (10 weeks of age), transplanted with human and rat hepatocytes, respectively, were prepared by PhoenixBio Co., Ltd. (Hiroshima, Japan). All animals were housed in a temperature- and humidity-controlled environment under a 12-h light/dark cycle with free access to tap water and food.

Human hepatocytes of a donor (African-American boy, 5 years old) were obtained from BD Biosciences (San Jose, CA). Rat hepatocytes for the preparation of r-PXB mice were isolated from the liver of Sprague-Dawley rats (4

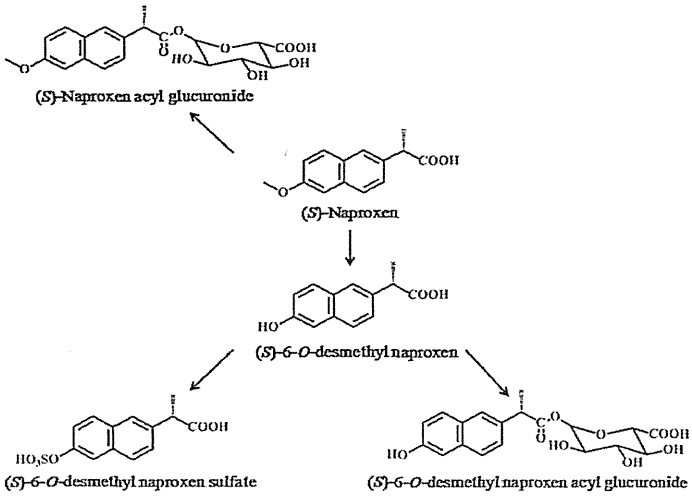

FIG. 2. Proposed metabolic pathways of (*S*)-naproxen in humans. This figure was drawn from the data of Sugawara et al. (1978).

weeks of age, male). The replacement ratio of host hepatocytes with human or rat hepatocytes, calculated as the replacement index (RI), was determined by measurement of the level of human or rat albumin in blood collected from the tail vein of each PXB mouse (Tateno et al., 2004; Emoto et al., 2005). Average RI values of h-PXB mice and r-PXB mice used in this study were 78 and nearly 100%, respectively.

Administration of Ibuprofen and (*S*)-Naproxen. Ibuprofen and (*S*)-naproxen solution (5 ml/kg) were administered orally to each animal at 20 and 10 mg/kg b.wt., respectively, which included 0.5% carboxymethylcellulose with a requisite minimum amount of potassium hydroxide for solution. After treatment of ibuprofen and (*S*)-naproxen, pooled urine samples were collected until 24 and 48 h, respectively.

Analysis and Quantitation of Ibuprofen, (*S*)-Naproxen, and Their Metabolites. *Ibuprofen.* Pooled urine (20 μl) was mixed with 0.1% formic acid (500 μl) and internal standard solution (30 μg/ml ketoprofen, 10 μl). These mixtures were absorbed to a MonoSpin C18 column (GL Sciences Inc., Tokyo, Japan) for solid-phase extraction. Samples purified by elution with 50% acetonitrile were subjected to liquid chromatography (LC)-tandem mass spectrometry (MS/MS). The concentrations of ibuprofen acyl glucuronide, carboxy ibuprofen acyl glucuronide and 2-hydroxyibuprofen acyl glucuronide were determined as increased amounts of ibuprofen, carboxy ibuprofen, and 2-hydroxyibuprofen by hydrolysis using 1 M sodium hydroxide before solid-phase extraction.

(S)-Naproxen. Pooled urine (20 μl) was mixed with acetonitrile (30 μl). After centrifugation, the supernatants with 10 mM ammonium acetate were subjected to LC-MS/MS.

The concentrations of (*S*)-6-*O*-desmethyl naproxen glucuronide were determined as increased amounts of 6-*O*-desmethyl naproxen by incubation for 2 h at 37°C using β-glucuronidase (20 μl) in 1 M acetate buffer (100 μl) after the hepatocytes were thawed. The concentration of 6-*O*-desmethyl naproxen sulfate was estimated by subtracting the concentration of 6-*O*-desmethyl naproxen glucuronide from that of total hydrolyzed 6-*O*-desmethyl naproxen after enzyme deconjugation for 2 h at 37°C using β-glucuronidase-arylsulfatase (20 μl) in 1 M acetate buffer. Incubation mixtures were extracted with ethyl acetate (5 ml) and internal standard solution (ketoprofen). The organic layer (4 ml) was evaporated to dryness, and the residues were dissolved in aqueous acetonitrile (100 μl). Aliquots of 10 μl were applied to the LC-MS/MS system.

LC-MS/MS conditions. Aliquots (10 μl) of urine samples were introduced into the LC system (Agilent Technologies, Santa Clara, CA). The mobile phase condition for ibuprofen and (*S*)-naproxen consisted of 10 mM ammonium acetate (A) and acetonitrile (B) through an Inersil ODS-3 column (5 μl, 50 × 2.1 mm; GL Sciences Inc.) at 40°C. The flow rate was set at 0.2 ml/min. The starting condition for the LC gradient was 90:10 (A/B). From 0 to 5 min, the mobile phase composition was changed to 10:90 (A/B), and this was maintained until 8 min. The gradient was then returned to 90:10 (A/B) linearly from 8 to 8.1 min, and the column was reequilibrated to the initial condition from 8.1 to 15 min. The elution times of ibuprofen, ibuprofen taurine conjugate, carboxy ibuprofen, 2-hydroxyibuprofen, (*S*)-naproxen, naproxen acyl glucuronide, (*S*)-6-*O*-desmethylnaproxen, and ketoprofen as internal standard were 5.9, 5.8, 0.9, 4.2, 5.0, 4.9, 4.0, and 5.0 min, respectively.

The MS/MS experiments were conducted by using API2000 LC-MS/MS systems (Applied Biosystems, Foster, CA). Mass numbers of the ionization mode, molecular ion, and product ion for ibuprofen, (*S*)-naproxen, and their metabolites were as follows: ibuprofen m/z = 204.9 $[M - H]^-$ to 158.5, ibuprofen taurine conjugate m/z = 311.9 $[M - H]^-$ to 123.4, carboxy ibuprofen m/z = 235.1 $[M - H]^-$ to 72.6, 2-hydroxyibuprofen m/z = 221.3 $[M - H]^-$ to 176.9, (*S*)-naproxen m/z = 228.7 $[M - H]^-$ to 168.5, naproxen acyl glucuronide m/z = 404.8 $[M - H]^-$ to 169.1, (*S*)-6-*O*-desmethylnaproxen m/z = 214.7 $[M - H]^-$ to 170.4, and ketoprofen m/z = 253.2 $[M - H]^-$ to 208.7.

Results

Predictability of Metabolic Profiles of Ibuprofen in Humans. Proposed metabolic pathways of ibuprofen were reported previously from the urinary metabolic profile excreted in humans after oral administration of ibuprofen (Fig. 1). Six metabolites, ibuprofen acyl glucuronide, ibuprofen taurine conjugate, carboxy ibuprofen, carboxy ibuprofen glucuronide, 2-hydroxyibuprofen, and 2-hydroxyibuprofen acyl glucuronide were predominantly detected in urine (Shirley et al., 1994; Kepp et al., 1997). The percentage values in Table 1 indicate urinary excreted metabolites in relation to the dose (percentage of dose) after oral administration of ibuprofen in humans (400 and 600 mg/person), h-PXB mice (20 mg/kg), rats (20 mg/kg), and r-PXB mice (20 mg/kg). These metabolites observed in humans were also identified in h-PXB mice, rats, and r-PXB mice. The amount of excreted unchanged form of ibuprofen in urine was negligible in all animals in this study (less than 2% of the dose). Amounts of excreted acyl glucuronide conjugates in human urine were higher than those of rats, whereas the amount of 2-hydroxyibuprofen in humans was lower than that of rats. We directly compared six urinary metabolites (percentage of dose) between humans and rats (Fig. 3A). There were weak correlations (r^2 = 0.471, p = 0.132). The correlations reflect species differences in the excretory metabolic profile between humans and rats. To investigate whether these differences reflect each chimeric mice, we directly compared the excreted metabolites between humans and h-PXB mice. This result showed good correlation (r^2 = 0.863, p = 0.007) (Fig. 3B). In addition, good correlation was also found between rats and r-PXB mice (r^2 = 0.928, p = 0.002) (Fig. 3C), whereas the relationship between h-PXB mice and r-PXB mice was weaker (r^2 = 0.286, p = 0.274) (Fig. 3D). These data suggested that the excretory metabolic profiles in humans and rats qualitatively reflected those of h-PXB mice and r-PXB mice, respectively. In a comparison with SCID mice, the host of chimeric mice, a low correlation was observed between humans and SCID mice (r^2 = 0.246, p = 0.317) and between h-PXB mice and SCID mice (r^2 = 0.129, p = 0.484) (Fig. 3, E and F).

Predictability of Metabolic Profiles of (*S*)-Naproxen in Humans. (*S*)-Naproxen is metabolized into four metabolites: (*S*)-naproxen acyl glucuronide, (*S*)-6-*O*-desmethylnaproxen, and the latter's metabolites, (*S*)-6-*O*-desmethylnaproxen sulfate and (*S*)-6-*O*-desmethylnaproxen

TABLE 1

Cumulative urinary excretion of six metabolites of ibuprofen

Human data (mean ± S.D., n = 4) after oral administration of ibuprofen (600 mg/person) are from Kepp et al. (1997). Data on the amount of ibuprofen taurine conjugate (mean ± S.E., n = 4) in humans after oral administration (400 mg/person) are from Shirley et al. (1994). Each value for h-PXB mice, r-PXB mice, rats, and SCID mice after oral administration (20 mg/kg) is the mean ± S.D. of n = 8, 3, 3, and 3 respectively.

Species	Urinary Excreted Metabolites					
	Ibuprofen Acyl Glucuronide	Ibuprofen Taurine Conjugate	Carboxy Ibuprofen	Carboxy Ibuprofen Glucuronide	2-Hydroxyibuprofen	2-Hydroxyibuprofen Acyl Glucuronide
			% dose			
h-PXB mice	11.3 ± 8.5	0.4 ± 0.4	5.4 ± 2.3	7.0 ± 3.4	2.4 ± 2.3	8.4 ± 4.7
Humans	11.6 ± 7.6	1.5 ± 0.5	13.5 ± 3.7	11.6 ± 7.3	5.9 ± 2.7	28.1 ± 8.5
r-PXB mice	0.9 ± 0.7	0.2 ± 0.2	4.4 ± 3.5	1.2 ± 1.1	8.8 ± 6.9	23.8 ± 17.4
Rats	0.2 ± 0.1	$8.0 \times 10^{-3} \pm 2.0 \times 10^{-3}$	2.9 ± 0.5	0.8 ± 0.6	34.5 ± 9.8	19.8 ± 2.4
SCID mice	2.5 ± 1.7	0.5 ± 0.3	5.3 ± 2.5	0.2 ± 4.3	1.5 ± 0.6	5.3 ± 2.8

acyl glucuronide, which were reported to be mainly excreted in the urine of humans (Fig. 2) (Sugawara et al., 1978). (*S*)-Naproxen was also excreted at negligible levels. Table 2 shows the percentage of each urinary metabolite after oral administration of (*S*)-naproxen in humans (200 mg/person), h-PXB mice (10 mg/kg), rats (10 mg/kg), and r-PXB mice (10 mg/kg). Four metabolites reported in humans were also found in the urine of h-PXB mice, rats, and r-PXB mice. Amounts of excreted naproxen acyl glucuronide and 6-*O*-desmethylnaproxen acyl glucuronide in human urine were higher than those of rats, whereas the amounts of 6-*O*-desmethylnaproxen and its sulfate in human were lower than that of rats.

We compared the percentages of dose of these excretory metabolites with those of chimeric mice. The amounts of naproxen acyl glucuronide, which was mainly observed in human urine and that of 6-desmethylnaproxen, the amount of which was low, corresponded to those of h-PXB mice. On the other hand, the amount of 6-*O*-desmethylnaproxen sulfate, which was mainly observed in rats, and that of naproxen acyl glucuronide, which was lower, were in close agreement with those of r-PXB mice. Differences in excretory metabolic profiles between humans and rats were similar to those between h-PXB mice and r-PXB mice.

Discussion

Identification of primary metabolites contributes to drug design for stable metabolic analogs. Not only primary metabolites but also secondary metabolites could be involved in efficacy and toxicity via biotransformation.

It is also necessary to reflect on species differences in isoform composition, expression, and activity of drug metabolic enzymes between humans and experimental animals (Martignoni et al., 2006). We considered that h-PXB mice with a high replacement of human hepatocytes may be useful for prediction of human metabolism because the expression levels and activities of both P450 and non-P450 enzymes reflect those of the donor hepatocytes (Yoshitsugu et al., 2006; Yamasaki et al., 2010). Sanoh et al. (2012a) demonstrated the predictability of human PK of 13 model compounds, including ibuprofen and (*S*)-naproxen, metabolized by P450 and non-P450, using h-PXB mice. For ibuprofen, the predictability of in vivo intrinsic clearance in h-PXB mice reflected that observed in humans (Sanoh et al., 2012a).

Ibuprofen was metabolized by CYP2C9 and UGT2B7 (Hamman et al., 1997; Buchheit et al., 2011). In addition, a taurine conjugate of ibuprofen was identified in the urine of humans as a minor metabolite (Shirley et al., 1994). (*S*)-Naproxen was metabolized by CYP2C9, CYP1A2, UGT2B7, and SULT1A1 (Rodrigues et al., 1996; Bowalgaha et al., 2005; Falany et al., 2005).

TABLE 2

Cumulative urinary excretion of four metabolites of (S)-naproxen

Human data (mean ± S.D., $n = 3$) after oral administration (200 mg/person) are from Sugawara et al. (1978). The amounts of acyl glucuronide formed were determined by hydrolysis with β-glucuronidase. The amount of sulfate of desmethyl naproxen was determined by hydrolysis with 2 N HCl (Sugawara et al., 1978). Data on metabolites of h-PXB mice, r-PXB mice, and rats after oral administration (10 mg/kg) are means ± S.D. of $n = 3$.

Species	Urinary Excreted Metabolites			
	(*S*)-Naproxen Acyl Glucuronide	(*S*)-6-*O*-Desmethyl Naproxen	(*S*)-6-*O*-Desmethyl Naproxen Acyl Glucuronide	(*S*)-6-*O*-Desmethylnaproxen Sulfate
	% dose			
h-PXB mice	26.5 ± 6.6	0.2 ± 0.2	1.0 ± 0.6	12.4 ± 3.1
Humans	25.3 ± 6.7	0.9 ± 0.2	8.3 ± 2.0	10.8 ± 0.5
r-PXB mice	2.9 ± 2.9	2.5 ± 1.4	0.5 ± 0.5	57.3 ± 6.1
Rats	1.2 ± 0.7	5.3 ± 3.8	1.8 ± 0.4	56.9 ± 8.7

CYP2C9 is one of the most abundant P450 enzymes in human liver. CYP2C9 metabolizes approximately 20% of clinical drugs, including a number of drugs with a narrow therapeutic ranges. UGT2B7 also contributes to the metabolism of numerous clinical drugs (Williams et al., 2004).

Ibuprofen and (*S*)-naproxen are suitable as representative model compounds to elucidate the predictability of multiple metabolic pathways associated with P450 and non-P450 using h-PXB mice. Metabolites of ibuprofen and (*S*)-naproxen were reported to be excreted in urine, which suggested that the kidneys are the main excretion route (Sugawara et al., 1978; Shirley et al., 1994; Kepp et al., 1997). Furthermore, we used r-PXB mice as a control model in consideration of species differences between humans and rats in this study.

Six metabolites of ibuprofen, which were identified in humans, were also found in the urine of h-PXB mice, r-PXB mice, and rats. On the other hand, fecal excretion of these metabolites was low (data not shown). These findings suggested that h-PXB mice reflected species differences of the main excretory pathways of cefmetazole (Okumura et al., 2007). We could confirm species differences in the amounts of urinary excretion of these metabolites between humans and rats because a weak correlation ($r^2 = 0.471$, $p = 0.132$) was observed, as shown in Fig. 3A. There were good correlations between humans and h-PXB mice ($r^2 = 0.863$, $p = 0.007$), as well as between rats and r-PXB mice ($r^2 = 0.928$, $p = 0.002$) (Fig. 3, B and C). Therefore, species differences in urinary excretion of metabolites between humans and rats reflect the relationship between h-PXB mice and r-PXB mice.

(*S*)-Naproxen is metabolized in humans by acyl glucuronidation, O-demethylation, and further sulfation and glucuronidation. Four metabolites were found in urine after administration in h-PXB mice, r-PXB mice, and rats. Species differences in excretory metabolites between humans and rats reflect the levels in humans and rats because amounts of each urinary metabolite were similar between humans and h-PXB mice as well as rats and r-PXB mice, in common with the results for ibuprofen.

We used h-PXB mice for which the average RI values were approximately 80%. The contribution of the remaining 20% of host hepatocytes may have influenced the predictability. Direct comparison of excretory metabolites between humans and SCID mice as host mice gave a value of $r^2 = 0.246$ ($p = 0.317$) (Fig. 3E). In addition, there was no correlation ($r^2 = 0.129$, $p = 0.484$) between h-PXB mice and SCID mice (Fig. 3F), although in vitro intrinsic clearance of ibuprofen in SCID mouse hepatocytes was similar to that of h-PXB mouse hepatocytes (Sanoh et al., 2012a). This result suggested that the remaining host mouse hepatocytes did not affect the predictability using h-PXB mice despite species differences between humans and SCID mice being observed. For r-PXB mice, it is not necessary to consider the remaining host mouse hepatocytes because RI of rat hepatocytes in liver of r-PXB mice is approximately 100%.

In this study, analysis of the predictability using h-PXB mice and r-PXB mice was conducted by oral administration. It is also necessary to consider the effects of the intestine, which is not humanized in h-PXB mice, in cases of oral administration. We compared recovery metabolites in h-PXB mice after intravenous and oral administration of ibuprofen. Because these results showed good correlation ($r^2 = 0.900$, $p = 0.004$), metabolic activities of ibuprofen in mouse intestine may be negligible (data not shown).

Our results using ibuprofen and (*S*)-naproxen indicated that in vivo metabolic activities of P450 and non-P450, such as those involving UGT, SULT, and amino acid *N*-acyltransferase in h-PXB mice and r-PXB mice, should be similar to those of humans and rats. In this study, r-PXB mice were used as the control animal for transplantation

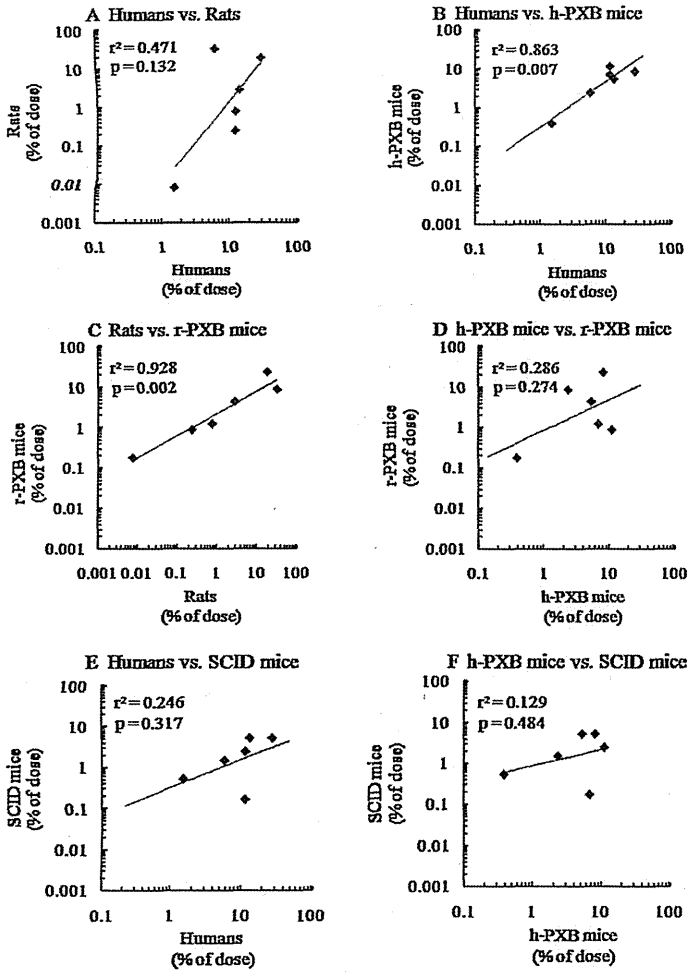

FIG. 3. Cross-species comparison of ibuprofen metabolites excreted in urine after oral administration of ibuprofen in h-PXB mice, humans, r-PXB mice, rats, and SCID mice. Comparison of each urinary excreted metabolite (percentage of dose) between (A) humans and rats, (B) humans versus h-PXB mice, (C) rats versus r-PXB mice, (D) h-PXB mice versus r-PXB mice, (E), humans versus SCID mice, and (F) h-PXB mice versus SCID mice.

of hepatocytes. Predictability using h-PXB mice may improve when the metabolic profiles of r-PXB mice reflect those of rats.

In conclusion, our results suggest that the combined use of h-PXB mice and r-PXB mice may be helpful for quantitative prediction of species differences of drug metabolism during the early stages of drug development in the pharmaceutical industry.

Acknowledgments

We thank colleagues at PhoenixBio Co., Ltd. (Hiroshima, Japan) for preparing PXB mice.

Authorship Contributions

Participated in research design: Sanoh, Sugihara, Kotake, Tayama, Horie, Kitamura, and Ohta.

Conducted experiments: Sanoh and Horiguchi.

Contributed new reagents or analytic tools: Sugihara, Kotake, Uramaru, Ohshita, and Tateno.

Performed data analysis: Sanoh and Horiguchi.

Wrote or contributed to the writing of the manuscript: Sanoh, Kotake, and Ohta.

References

Anderson S, Luffer-Atlas D, and Knadler MP (2009) Predicting circulating human metabolites: how good are we? *Chem Res Toxicol* **22**:243–256.

Bowalgaha K, Elliot DJ, Mackenzie PI, Knights KM, Swedmark S, and Miners JO (2005) *S*-Naproxen and desmethylnaproxen glucuronidation by human liver microsomes and recombinant human UDP-glucuronosyltransferases (UGT): role of UGT2B7 in the elimination of naproxen. *Br J Clin Pharmacol* **60**:423–433.

Brown HS, Griffin M, and Houston JB (2007) Evaluation of cryopreserved human hepatocytes as an alternative in vitro system to microsomes for the prediction of metabolic clearance. *Drug Metab Dispos* **35**:293–301.

Buchheit D, Dragan CA, Schmitt EI, and Bureik M (2011) Production of ibuprofen acyl glucosides by human UGT2B7. *Drug Metab Dispos* **39**:2174–2181.

Chiba M, Ishii Y, and Sugiyama Y (2009) Prediction of hepatic clearance in human from in vitro data for successful drug development. *AAPS J* **11**:262–276.

Dalvie D, Obach RS, Kang P, Prakash C, Loi CM, Hurst S, Nedderman A, Goulet L, Smith E, Bu HZ, et al. (2009) Assessment of three human in vitro systems in the generation of major human excretory and circulating metabolites. *Chem Res Toxicol* **22**:357–368.

De Serres M, Bowers G, Boyle G, Beaumont C, Castellino S, Sigafoos J, Dave M, Roberts A, Shah V, Olson K, et al. (2011) Evaluation of a chimeric (uPA$^{+/+}$)/SCID mouse model with a humanized liver for prediction of human metabolism. *Xenobiotica* **41**:464–475.

Emoto K, Tateno C, Hino H, Amano H, Imaoka Y, Asahina K, Asahara T, and Yoshizato K (2005) Efficient *in vivo* xenogeneic retroviral vector-mediated gene transduction into human hepatocytes. *Hum Gene Ther* **16**:1168–1174.

Falany CN, Ström P, and Swedmark S (2005) Sulphation of *O*-desmethylnaproxen and related compounds by human cytosolic sulfotransferases. *Br J Clin Pharmacol* **60**:632–640.

Fagerholm U (2007) Prediction of human pharmacokinetics—evaluation of methods for prediction of hepatic metabolic clearance. *J Pharm Pharmacol* **59**:803–828.

Hallifax D, Foster JA, and Houston JB (2010) Prediction of human metabolic clearance from in vitro systems: retrospective analysis and prospective view. *Pharm Res* **27**:2150–2161.

Hamman MA, Thompson GA, and Hall SD (1997) Regioselective and stereoselective metabolism of ibuprofen by human cytochrome P450 2C. *Biochem Pharmacol* **54**:33–41.

Inoue T, Sugihara K, Ohshita H, Horie T, Kitamura S, and Ohta S (2009) Prediction of human disposition toward *S*-^{3}H-warfarin using chimeric mice with humanized liver. *Drug Metab Pharmacokinet* **24**:153–160.

Katoh M, Matsui T, Nakajima M, Tateno C, Kataoka M, Soeno Y, Horie T, Iwasaki K, Yoshizato

K, and Yokoi T (2004) Expression of human cytochromes P450 in chimeric mice with humanized liver. *Drug Metab Dispos* **32:**1402–1410.
Katoh M, Matsui T, Okumura H, Nakajima M, Nishimura M, Naito S, Tateno C, Yoshizato K, and Yokoi T (2005) Expression of human phase II enzymes in chimeric mice with humanized liver. *Drug Metab Dispos* **33:**1333–1340.
Katoh M and Yokoi T (2007) Application of chimeric mice with humanized liver for predictive ADME. *Drug Metab Rev* **39:**145–157.
Kepp DR, Sidelmann UG, Tjørnelund J, and Hansen SH (1997) Simultaneous quantitative determination of the major phase I and II metabolites of ibuprofen in biological fluids by high-performance liquid chromatography on dynamically modified silica. *J Chromatogr B Biomed Sci Appl* **696:**235–241.
Kitamura S, Nitta K, Tayama Y, Tanoue C, Sugihara K, Inoue T, Horie T, and Ohta S (2008) Aldehyde oxidase-catalyzed metabolism of N1-methylnicotinamide in vivo and in vitro in chimeric mice with humanized liver. *Drug Metab Dispos* **36:**1202–1205.
Kola I and Landis J (2004) Can the pharmaceutical industry reduce attrition rates? *Nat Rev Drug Discov* **3:**711–715.
Martignoni M, Groothuis GM, and de Kanter R (2006) Species differences between mouse, rat, dog, monkey and human CYP-mediated drug metabolism, inhibition and induction. *Expert Opin Drug Metab Toxicol* **2:**875–894.
Mills RF, Adams SS, Cliffe EE, Dickinson W, and Nicholson JS (1973) The metabolism of ibuprofen. *Xenobiotica* **3:**589–598.
Nagilla R, Frank KA, Jolivette LJ, and Ward KW (2006) Investigation of the utility of published in vitro intrinsic clearance data for prediction of in vivo clearance. *J Pharmacol Toxicol Methods* **53:**106–116.
Nishimura M, Yoshitsugu H, Yokoi T, Tateno C, Kataoka M, Horie T, Yoshizato K, and Naito S (2005) Evaluation of mRNA expression of human drug-metabolizing enzymes and transporters in chimeric mouse with humanized liver. *Xenobiotica* **35:**877–890.
Obach RS, Baxter JG, Liston TE, Silber BM, Jones BC, MacIntyre F, Rance DJ, and Wastall P (1997) The prediction of human pharmacokinetic parameters from preclinical and in vitro metabolism data. *J Pharmacol Exp Ther* **283:**46–58.
Okumura H, Katoh M, Sawada T, Nakajima M, Soeno Y, Yabuuchi H, Ikeda T, Tateno C, Yoshizato K, and Yokoi T (2007) Humanization of excretory pathway in chimeric mice with humanized liver. *Toxicol Sci* **97:**533–538.
Rodrigues AD, Kukulka MJ, Roberts EM, Ouellet D, and Rodgers TR (1996) [*O-methyl* ^{14}C]naproxen *O*-demethylase activity in human liver microsomes: evidence for the involvement of cytochrome P4501A2 and P4502C9/10. *Drug Metab Dispos* **24:**126–136.
Sanoh S, Horiguchi A, Sugihara K, Kotake Y, Tayama Y, Ohshita H, Tateno C, Horie T, Kitamura S, and Ohta S (2012a) Prediction of *in vivo* hepatic clearance and half-life of drug candidates in human using chimeric mice with humanized liver. *Drug Metab Dispos* **40:**322–328.
Sanoh S, Nozaki K, Murai H, Terashita S, Teramura T, and Ohta S (2012b) Prediction of human metabolism of FK3453 by aldehyde oxidase using chimeric mice transplanted with human or rat hepatocytes. *Drug Metab Dispos* **40:**76–82.
Shirley MA, Guan X, Kaiser DG, Halstead GW, and Baillie TA (1994) Taurine conjugation of ibuprofen in humans and in rat liver *in vitro*. Relationship to metabolic chiral inversion. *J Pharmacol Exp Ther* **269:**1166–1175.
Stringer R, Nicklin PL, and Houston JB (2008) Reliability of human cryopreserved hepatocytes and liver microsomes as in vitro systems to predict metabolic clearance. *Xenobiotica* **38:**1313–1329.
Sugawara Y, Fujihara M, Miura Y, Hayashida K, and Takahashi T (1978) Studies on the fate of naproxen. II. Metabolic fate in various animals and man. *Chem Pharm Bull* **26:**3312–3321.
Tateno C, Yoshizane Y, Saito N, Kataoka M, Utoh R, Yamasaki C, Tachibana A, Soeno Y, Asahina K, Hino H, et al. (2004) Near completely humanized liver in mice shows human-type metabolic responses to drugs. *Am J Pathol* **165:**901–912.
Yamasaki C, Kataoka M, Kato Y, Kakuni M, Usuda S, Ohzone Y, Matsuda S, Adachi Y, Ninomiya S, Itamoto T, et al. (2010) In vitro evaluation of cytochrome P450 and glucuronidation activities in hepatocytes isolated from liver-humanized mice. *Drug Metab Pharmacokinet* **25:**539–550.
Yamazaki H, Kuribayashi S, Inoue T, Tateno C, Nishikura Y, Oofusa K, Harada D, Naito S, Horie T, and Ohta S (2010) Approach for *in vivo* protein binding of 5-*n*-butyl-pyrazolo[1,5-*a*]pyrimidine bioactivated in chimeric mice with humanized liver by two-dimensional electrophoresis with accelerator mass spectrometry. *Chem Res Toxicol* **23:**152–158.
Yoshitsugu H, Nishimura M, Tateno C, Kataoka M, Takahashi E, Soeno Y, Yoshizato K, Yokoi T, and Naito S (2006) Evaluation of human CYP1A2 and CYP3A4 mRNA expression in hepatocytes from chimeric mice with humanized liver. *Drug Metab Pharmacokinet* **21:**465–474.
Williams JA, Hyland R, Jones BC, Smith DA, Hurst S, Goosen TC, Peterkin V, Koup JR, and Ball SE (2004) Drug-drug interactions for UDP-glucuronosyltransferase substrates: a pharmacokinetic explanation for typically observed low exposure (AUC_i/AUC) ratios. *Drug Metab Dispos* **32:**1201–1208.

Address correspondence to: Dr. Seigo Sanoh, Graduate School of Biomedical and Health Sciences, Hiroshima University, Kasumi 1-2-3, Minami-ku, Hiroshima 734-8553, Japan. E-mail:sanoh@hiroshima-u.ac.jp

1521-009X/12/4002-322–328$25.00
DRUG METABOLISM AND DISPOSITION
Vol. 40, No. 2
40923/3743170
DMD 40:322–328, 2012

Prediction of In Vivo Hepatic Clearance and Half-Life of Drug Candidates in Human Using Chimeric Mice with Humanized Liver[S]

Seigo Sanoh, Aya Horiguchi, Kazumi Sugihara, Yaichiro Kotake, Yoshitaka Tayama, Hiroki Ohshita, Chise Tateno, Toru Horie, Shigeyuki Kitamura, and Shigeru Ohta

Graduate School of Biomedical Sciences (S.S., A.H., Y.K., S.O.) and Liver Research Project Center, Hiroshima University, Hiroshima, Japan (C.T.); Faculty of Pharmaceutical Sciences, Hiroshima International University, Hiroshima, Japan (K.S., Y.T.); PXB Mouse Production Department (H.O.) and R&D Department (C.T.), PhoenixBio Co., Ltd., Hiroshima, Japan; DeThree Research Laboratories, Ibaraki, Japan (T.H.); and Nihon Pharmaceutical University, Saitama, Japan (S.K.)

Received August 5, 2011; accepted November 2, 2011

ABSTRACT:

Accurate prediction of pharmacokinetics (PK) parameters in humans from animal data is difficult for various reasons, including species differences. However, chimeric mice with humanized liver (PXB mice; urokinase-type plasminogen activator/severe combined immunodeficiency mice repopulated with approximately 80% human hepatocytes) have been developed. The expression levels and metabolic activities of cytochrome P450 (P450) and non-P450 enzymes in the livers of PXB mice are similar to those in humans. In this study, we examined the predictability for human PK parameters from data obtained in PXB mice. Elimination of selected drugs involves multiple metabolic pathways mediated not only by P450 but also by non-P450 enzymes, such as UDP-glucuronosyltransferase, sulfotransferase, and aldehyde oxidase in liver. Direct comparison between in vitro intrinsic clearance ($CL_{int,in\ vitro}$) in PXB mice hepatocytes and in vivo intrinsic clearance ($CL_{int,in\ vivo}$) in humans, calculated based on a well stirred model, showed a moderate correlation ($r^2 = 0.475$, $p = 0.009$). However, when $CL_{int,in\ vivo}$ values in humans and PXB mice were compared similarly, there was a good correlation ($r^2 = 0.754$, $p = 1.174 \times 10^{-4}$). Elimination half-life ($t_{1/2}$) after intravenous administration also showed a good correlation ($r^2 = 0.886$, $p = 1.506 \times 10^{-4}$) between humans and PXB mice. The rank order of CL and $t_{1/2}$ in human could be predicted at least, although it may not be possible to predict absolute values due to rather large prediction errors. Our results indicate that in vitro and in vivo experiments with PXB mice should be useful at least for semiquantitative prediction of the PK characteristics of candidate drugs in humans.

Introduction

It is important to predict human pharmacokinetics (PK) and metabolism of drug candidates in the preclinical stage of pharmaceutical development. Various approaches to predict human clearance (CL) with in vitro metabolic systems, such as human liver microsomes and hepatocytes, have been reported (Nagilla et al., 2006; Brown et al., 2007; Fagerholm, 2007; Stringer et al., 2008; Chiba et al., 2009; Hallifax et al., 2010) but with limited success. One of the reasons for the discrepancy between predicted and observed CL may be that the preparation, storage, and experimental treatment of hepatocytes alter the normal function of metabolic enzymes (Wang et al., 2005). Although this might be ameliorated by using fresh hepatocytes immediately after isolation from the liver, these are not readily available and in any case show considerable interindividual differences.

It has become possible recently to predict CL and half-life ($t_{1/2}$) by means of computational approaches and physiologically based modeling (Ekins and Obach, 2000; De Buck et al., 2007; Tabata et al., 2009; Paixão et al., 2010). Accurate prediction of human PK is a key issue for the development of new drugs, because many new drug candidates with diverse chemical structures are metabolized not only by cytochrome P450 (P450) but also by non-P450 enzymes, such as UDP-glucuronosyltransferase (UGT) and sulfotransferase (SULT). It is also necessary to take into account the effects of cell permeability, transporter-mediated uptake, and excretion (Chiba et al., 2009; Huang et al., 2010).

Chimeric mice with humanized liver (PXB mice; PhoenixBio Co., Ltd., Hiroshima, Japan) have been generated from urokinase-type plasminogen activator/severe combined immunodeficiency mice transplanted with human hepatocytes (Tateno et al., 2004). In these mice, approximately 80% of the hepatocytes are human. The expression levels and metabolic activities of P450 and non-P450 enzymes in

This work was supported by a Grant-in-Aid for Young Scientists (B) from Japan Society for the Promotion of Science [Grant 22790109]; and PhoenixBio, Co., Ltd.

Article, publication date, and citation information can be found at http://dmd.aspetjournals.org.

http://dx.doi.org/10.1124/dmd.111.040923.

[S] The online version of this article (available at http://dmd.aspetjournals.org) contains supplemental material.

ABBREVIATIONS: PK, pharmacokinetics; CL, clearance; AO, aldehyde oxidase; $CL_{int,in\ vitro}$, in vitro intrinsic clearance; $CL_{int,in\ vivo}$, in vitro intrinsic clearance; CL_{oral}, oral clearance; CL_t, total clearance; P450, cytochrome P450; DMSO, dimethyl sulfoxide; fu, plasma unbound fraction; h-hepatocytes, PXB mice hepatocytes; LC/MS/MS, liquid chromatography tandem mass spectrometry; NAT, *N*-acetyltransferase; PXB mice, chimeric mice with humanized liver; Q, hepatic blood flow; Rb, blood/plasma concentration ratio; RI, replacement index; SULT, sulfotransferase; $t_{1/2}$, half-life; UGT, UDP-glucuronosyltransferase; AUC_{iv}, area under the concentration versus time curve by intravenous administration.

livers of PXB mice with a high replacement index (RI) are similar to those of humans (Katoh et al., 2004, 2005), and human-specific metabolites are formed in PXB mice (Inoue et al., 2009; Kamimura et al., 2010; Yamazaki et al., 2010; De Serres et al., 2011). Thus, PXB mice could be a good in vivo model for predicting drug metabolism in humans.

However, quantitative methods for predicting PK parameters of humans from data in PXB mice have not been established yet. Therefore, we selected 13 model compounds that are metabolized by P450 and/or non-P450 enzymes in liver and compared the PK parameters in humans and PXB mice, using both in vitro and in vivo approaches, to evaluate the utility of this animal model for the prediction of human PK.

Materials and Methods

Chemicals. 6-Deoxypenciclovir and mirtazapine were obtained from Toronto Research Chemicals Inc. (North York, ON, Canada). Dapsone, lamotrigine, salbutamol, and sulindac were purchased from Sigma-Aldrich (St. Louis, MO). Diclofenac was purchased from Tokyo Chemical Industry Co. Ltd. (Tokyo, Japan). Fasudil was obtained from Tocris Bioscience (Bristol, UK). (*S*)-Naproxen was purchased from Cayman Chemical (Ann Arbor, MI). Ibuprofen, ketoprofen, and (*S*)-warfarin were purchased from Wako Pure Chemicals (Osaka, Japan). Zaleplon was kindly provided by King Pharm. Inc. (Bristol, UK). All of the other regents and solvents were commercial products of the highest available grade or analytical grade.

Animals. The present study was approved by the animal ethics committee and was conducted in accordance with the regulations on the use of living modified organisms of Hiroshima University. PXB mice (10–14 weeks of age) with human hepatocytes were prepared by the reported method (Tateno et al., 2004). Human hepatocytes of a donor (African-American boy, 5 years old) were obtained from BD Biosciences (San Jose, CA). PXB mice were housed in a temperature- and humidity-controlled environment under a 12-h light/dark cycle.

The RI was determined by the measurement of human albumin in blood collected from the tail vein. The RI was estimated by the correlation curve between the human albumin levels in mouse blood and determined by using human-specific cytokeratin 8/18-immunostained liver sections (Tateno et al., 2004). The RI values of PXB mice used in this study ranged from 73.4 to 93.4%.

Administration. Drug solution (5 ml/kg) was administered intravenously to PXB mice at 0.3 to 5 mg/kg body weight. Solutions of dapsone, diclofenac, 6-deoxypenciclovir, fasudil, ketoprofen, ibuprofen, mirtazapine, naproxen, salbutamol, and sulindac were prepared in saline. In the cases of ketoprofen, ibuprofen, naproxen, and sulindac, equivalent amounts of alkali were added. Dapsone solutions contained 10% dimethyl sulfoxide (DMSO), and mirtazapine solutions were prepared with 10% DMSO and equivalent amounts of hydrochloric acid. Lamotrigine, and zaleplon solutions were prepared with 10% DMSO and 10% polyethylene glycol 400 in saline. Equivalent amounts of hydrochloric acid also were added to the solutions of lamotrigine and zaleplon. Warfarin was formulated in 3% DMSO and 97% saline with an equivalent amount of sodium hydroxide.

Blood samples after dosing were collected from orbital veins of PXB mice at predetermined times using heparinized glass. These samples were centrifuged, and the plasma was stored at −30°C.

Determination of Drug Concentrations in Plasma. A 10 μl aliquot of plasma was added to 40 μl of acetonitrile or methanol containing an internal standard (carbamazepine, ketoprofen, or ibuprofen). The mixtures were centrifuged at 14,000*g* for 5 min, and the supernatant was subjected to liquid chromatography tandem mass spectrometry (LC/MS/MS).

Isolation and Purification of Hepatocytes from PXB Mice. Fresh hepatocytes were isolated from PXB mice (13–15 weeks of age) by means of the in situ collagenase perfusion method and purified as described previously (Yamasaki et al., 2010). PXB mouse hepatocytes (h-hepatocytes) contained approximately 7% mouse hepatocytes. We used h-hepatocytes purified by the use of 66Z rat IgG and magnetic beads bearing anti-rat IgG antibodies. The magnetic removal of mouse hepatocytes reduced the level of mouse hepatocytes to approximately 2% (in this study, the purity of human hepatocytes from PXB mouse hepatocytes ranged from 96.6 to 99.7% after purification). Cell viability of the hepatocytes used in the experiments ranged from 79 to 91%, as determined by means of the trypan blue exclusion test.

In Vitro Metabolic Studies Using h-Hepatocytes. The h-hepatocyte suspension (1×10^6 cells/ml) was incubated in Krebs-Henseleit buffer without serum in the presence of 10 μM of the test drug at 37°C under an atmosphere of 5% CO_2/95% O_2. The final concentration of acetonitrile was 0.5% (v/v) in the reaction mixture. The plates (24 wells) were shaken gently with an orbital shaker. The incubation mixture was sampled at 0, 0.25, 0.5, 1, and 2 h after treatment, and reactions were stopped by freezing the mixture in liquid nitrogen. When required, the samples were thawed, spiked with two volumes of acetonitrile or methanol containing an internal standard, and centrifuged. Aliquots of the supernatants were subjected to LC/MS/MS.

LC/MS/MS Conditions. Aliquots (10 μl) of plasma and h-hepatocyte suspension were introduced into the high-performance liquid chromatography system with an autosampler (Agilent Technologies, Santa Clara, CA). Several mobile phase conditions were used. Mobile phase condition 1 consisted of 10 mM ammonium acetate (A) and acetonitrile (B) on an Inertsil ODS-3 column (3 μm, 50 × 2.1 mm; GL Sciences Inc., Tokyo, Japan) at 40°C for the analysis of diclofenac, ibuprofen, ketoprofen, mirtazapine, (*S*)-naproxen, sulindac, and (*S*)-warfarin. The flow rate was set at 0.2 ml/min. The starting condition for the high-performance liquid chromatography gradient was 90:10 (A/B). From 0 to 5 min, the mobile phase composition was changed linearly to 10:90 (A/B), and this was held until 8 min. The gradient then was returned to 90:10 (A/B)

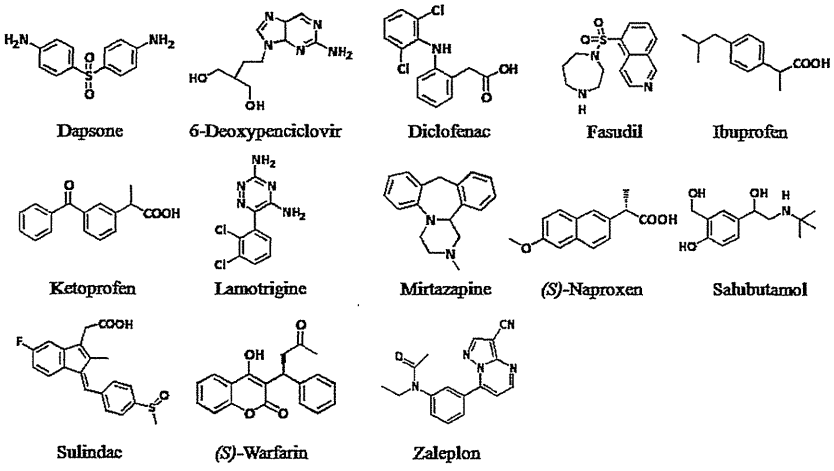

FIG. 1. Chemical structures of the model compounds used in this study.

TABLE 1

Literature values of plasma clearance, half-life, unbound fraction in plasma, blood/plasma concentration ratio, and metabolic enzymes in humans for the model compounds examined in this analysis

Rb values of fasudil, lamotrigine, and sulindac were assumed to be 1 due to unavailable data from the literature. References are in Supplemental Tables 1 and 2.

Compounds	CL_t or CL_{oral}	$t_{1/2}$	fu	Rb	Metabolic Enzymes
	$ml \cdot min^{-1} \cdot kg^{-1}$	h			
Dapsone	0.48	22	0.25	1.04	CYP2C9, CYP3A4, NAT
6-Deoxypenciclovir*,†	118	–	1	1.2	AO
Diclofenac	3.5	1.4	0.005	0.55	CYP2C9, UGT2B7, UGT1A9
Fasudil	73.2	0.26	0.51	1	AO
Ibuprofen	0.82	1.6	0.006	0.55	CYP2C9, UGT2B7
Ketoprofen	1.6	2.1	0.008	0.55	UGT2B7
Lamotrigine*	0.3	–	0.45	1	UGT1A4, UGT2B7
Mirtazapine	8.0	15	0.15	0.67	CYP1A2, CYP2D6, CYP3A4
(*S*)-Naproxen	0.1	–	0.01	0.55	CYP2C9, CYP1A2, UGT2B7
Salbutamol	7.7	3.9	0.925	0.96	SULT1A3
Sulindac*	3.3	–	0.069	1	AO
(*S*)-Warfarin	0.055	29	0.015	0.55	CYP2C9
Zaleplon	16	1.1	0.4	0.99	AO, CYP3A4

* From oral administration data.
† Calculated as famciclovir, which is prodrug of 6-deoxypenciclovir.
–, Unavailable data from intravenous administration.

linearly from 8 to 8.1 min, and the column was re-equilibrated to the initial condition.

Mobile phase condition 2 consisted of 0.1% formic acid (A) and methanol (B) on a YMC-Triart C18 column (3 μm, 50 × 2.1 mm; YMC Co., Ltd., Kyoto, Japan) for the analysis of dapsone, 6-deoxypenciclovir, fasudil, lamotrigine, salbutamol, and zaleplon. The starting condition was 90:10 (A/B). From 0 to 5 min, the mobile phase composition was changed linearly to 10:90 (A/B), and this was maintained until 8 min, then the column was re-equilibrated to the initial condition.

The MS/MS experiments were conducted by using API2000 LC/MS/MS systems (Applied Biosystems, Foster, CA). Mass number of the ionization mode, molecular ion, and product ion for the model compounds were as follows: dapsone m/z = 248.99 $[M + H]^+$ to 92.18, 6-deoxypenciclovir m/z = 238.05 $[M + H]^+$ to 210.95, diclofenac m/z = 294.14 $[M + H]^-$ to 249.53, fasudil m/z = 292.07 $[M + H]^+$ to 99.09, ibuprofen m/z = 204.88 $[M + H]^-$ to 158.52, ketoprofen m/z = 253.16 $[M + H]^-$ to 208.73, lamotrigine m/z = 256.03 $[M + H]^+$ to 210.96 mirtazapine m/z = 266.14 $[M + H]^+$ to 194.97, (*S*)-naproxen m/z = 228.68 $[M + H]^-$ to 168.55, salbutamol m/z = 240.18 $[M + H]^+$ to148.03, sulindac m/z = 357.07 $[M + H]^+$ to 232.96, (*S*)-warfarin m/z = 309.06 $[M + H]^+$ to162.97, zaleplon m/z = 306.08 $[M + H]^+$ to 236.12.

Determination of PK Parameters. Pharmacokinetic parameters were determined by noncompartmental methods using the concentration-time curve profile. The total clearances (CL_t) after intravenous administration were calculated as dose/AUC_{iv}. AUC_{iv} values were estimated from the time course using the trapezoidal method with extrapolation from the last quantifiable point to infinity. The terminal elimination $t_{1/2}$ was estimated as ln 2/*ke*, where *ke* is that of the plot of the terminal elimination phase on a logarithmic scale.

Calculation of In Vitro Intrinsic Clearance. In vitro intrinsic clearance ($CL_{int,in\ vitro}$) was calculated from the time course of the disappearance of the test drug during incubation with h-hepatocytes. Each plot was fitted to the first-order elimination rate constant as $C(t) = C_0 * \exp(-ke * t)$, where $C(t)$ and C_0 are the concentration of unchanged test drug at incubation time t and that at preincubation and *ke* is the disappearance rate constant of the unchanged drug.

Subsequently, $CL_{int,in\ vitro}$ ($\mu l \cdot min^{-1} \cdot 10^6\ cells^{-1}$) values were converted to $CL_{int,in\ vitro}$ ($ml \cdot min^{-1} \cdot kg^{-1}$) for the whole body. $CL_{int,in\ vitro}$ data were scaled up using physiological parameters, human liver weight 26 g/kg (Davies and Morris, 1993) and PXB mouse liver weight 140 g/kg, and the hepatocellularity (132 × 10^6 cells/g liver) of PXB mice. These parameters were taken from the average of observed data in PXB mice (RI = 80%).

Calculation of In Vivo Intrinsic Clearance. CL_t of PXB mice was calculated from the plasma concentrations after dosing using noncompartmental methods as described. CL_t was assumed to be equal to the hepatic clearance.

Values of CL_t, plasma unbound fraction (fu), and blood/plasma concentration ratio (Rb) in humans were taken from the literature.

In vivo intrinsic clearance ($CL_{int,in\ vivo}$) was calculated from the in vivo CL_t, fu, Rb, and average hepatic blood flow (Q) based on a well stirred model as $CL_{int,in\ vivo} = CL_t/\{(fu/Rb) \times (1 - CL_t/Q)\}$ (Pang and Rowland, 1977). These CL_t values were converted to blood clearance using Rb values.

The Q values of humans and PXB mice were set at 21 and 90 $ml \cdot min^{-1} \cdot kg^{-1}$ (same as in normal mice), respectively (Davies and Morris, 1993). In addition, Rb and fu of human were assumed to be equivalent to those of PXB mice. If CL_t of drugs exceeded liver blood flow, then the hepatic clearance was taken as 90% of liver blood flow. $CL_{int,in\ vivo}$ of 6-deoxypenciclovir, lamotrigine, and sulindac were evaluated from oral clearance (CL_{oral}) as CL_{oral}/fu/Rb.

Results

Selection of the Model Compounds for Analysis. In this study, we selected 13 compounds with diverse chemical structures (Fig. 1); Elimination of these selected drugs involves multiple metabolic pathways mediated not only by P450 but also by non-P450 enzymes, such as UGT, SULT, and aldehyde oxidase (AO) in liver. Mirtazapine and warfarin were known to be mainly metabolized by P450. Diclofenac, ibuprofen, and naproxen were metabolized by both UGT and P450. Furthermore, the model compounds metabolized by AO, such as

TABLE 2

Estimation of $CL_{int,in\ vitro}$ ($\mu l \cdot min^{-1} \cdot 10^6\ cells^{-1}$) in PXB mice hepatocytes and scaling to humans and PXB mice

$CL_{int,in\ vitro}$ ($\mu l \cdot min^{-1} \cdot 10^6\ cells^{-1}$) values were converted to $CL_{int,in\ vitro}$ ($ml \cdot min^{-1} \cdot kg^{-1}$) for the whole body. $CL_{int,in\ vitro}$ data were scaled up using physiological parameters, human liver weight (26 g/kg) and PXB mouse liver weight (140 g/kg), and the hepatocellularity (132 × 10^6 cells/g liver) of PXB mice. Each value represents the mean ± S.D. (n = 3).

Compounds	$CL_{int,in\ vitro}$	Scaled $CL_{int,in\ vitro}$ (Human)	Scaled $CL_{int,in\ vitro}$ (PXB Mice)
	$\mu l \cdot min^{-1} \cdot 10^6\ cells^{-1}$	$ml \cdot min^{-1} \cdot kg^{-1}$	
Dapsone	2.3 ± 1.2	8.0 ± 4.0	43.1 ± 21.3
6-Deoxypenciclovir	5.3 ± 1.2	18.3 ± 4.2	98.6 ± 22.4
Diclofenac	24.7 ± 1.2	84.7 ± 4.0	455.8 ± 21.3
Fasudil	35.7 ± 13.3	122.4 ± 45.6	659.1 ± 245.4
Ibuprofen	13.3 ± 2.1	45.8 ± 7.1	246.4 ± 38.5
Ketoprofen	6.0 ± 1.0	20.6 ± 3.4	110.9 ± 18.5
Lamotrigine	1.4 ± 1.0	4.8 ± 3.6	25.9 ± 19.2
Mirtazapine	6.3 ± 1.2	21.7 ± 4.0	117.0 ± 21.3
(*S*)-Naproxen	12.7 ± 2.5	43.5 ± 8.6	234.1 ± 46.5
Salbutamol	1.0 ± 1.0	3.3 ± 3.3	17.9 ± 17.8
Sulindac	2.0 ± 2.0	7.0 ± 6.7	37.6 ± 36.0
(*S*)-Warfarin	1.2 ± 0.7	4.1 ± 2.5	22.2 ± 13.3
Zaleplon	2.3 ± 1.2	8.0 ± 4.0	43.1 ± 21.3